

Article

Diversity and Functional Potential of Soil Bacterial Communities in Different Types of Farmland Shelterbelts in Mid-Western Heilongjiang, China

Jun Zhang , Ying Xin and Yusen Zhao *

College of Forestry, Northeast Forestry University, Harbin 150040, China; zhangjun@nefu.edu.cn (J.Z.); xinying2004@126.com (Y.X.)

* Correspondence: zhaoy1957@163.com; Tel.: +86-0451-85992066

Received: 1 November 2019; Accepted: 5 December 2019; Published: 6 December 2019



Abstract: The diversity and function of surface soil bacterial community in farmland shelterbelts of five forest types and one abandoned wilderness area were analyzed by collecting 36 soil samples at depths of 0–10 cm (the upper soil layer) and 10–20 cm (the lower soil layer), extracting DNA from the samples and amplifying and sequencing the bacterial 16S rDNA V3~V4 region. Dominant bacterial phyla in forest soils included the Actinomycetes, Proteobacteria, Acidobacteria, Chlorobacteria, and Bacillus. The number of unique bacterial OTUs (operational taxonomic units) was higher in the upper versus lower soil layer and greater in the abandoned cropland than in the shelterbelts. The number of total bacterial OTUs was highest in the mixed *Pinus sylvestris* var. *mongholica* Litv. and *Larix gmelinii* (Rupr.) Kuzen. forest. At the phyla level, Actinomycetes showed the greatest variation in abundance among forest types, while at the genus level, *Actinoplanes* varied most among forest types in the upper soil layer and *Krasilnikovia* varied most in the lower soil layer. Soil bacteria were more strongly correlated and more intense competition in the upper soil layer than in the lower soil layer; *Actinoplanes* and *Krasilnikovia* were key genera in bacterial networks. Functional predictions for bacterial community genes indicated that soil fertility potential was strong in the mixed *Fraxinus mandshurica* Rupr. and *Larix gmelinii* (Rupr.) Kuzen. forest, weak in the mixed *Pinus sylvestris* var. *mongholica* Litv. and *Larix gmelinii* (Rupr.) Kuzen. forest, and in the *Populus xiaohei* forest, and intermediate in the *Larix gmelinii* (Rupr.) Kuzen. and *Pinus sylvestris* var. *mongholica* Litv. forests. This study provides a new theoretical basis for the sustainable management of soil fertility in the agroforestry system.

Keywords: farmland shelterbelts; agroforestry system; 16S rDNA; high-throughput sequencing; bacterial diversity; community function prediction

1. Introduction

Farmland shelterbelts, an important part of agroforestry systems, are key ecological barriers against severe environmental conditions in northern China, which improve the microclimate of farmland and ensure high and stable crop yields [1]. Meanwhile, soils in agroforestry systems provide the necessary substrate for the survival and development of farmland shelterbelts. Forest surface soils represent an important habitat for microorganisms, many of which are beneficial and act to enhance nutrient absorption and retention [2,3]. Studies have shown that soil microorganisms can, to some extent, influence plant communities: for example, affecting drought tolerance and hormone levels [4,5], regulating biomass [6], altering reproductive phenology [7], and promoting lignin synthesis and metabolism [8].

Forest root systems interact in complex ways with soil microbial communities [9]. For example, the characteristics of the soil microbial community can respond to changes in soil ecological processes

and vegetation cover [10]. In most cases, the Eubacteria dominate soil microbial communities [11,12]. Soil bacteria are so valued because these microbial groups have the highest abundance and widest distribution in soils [13]. They play important roles in the decomposition of organic matter, the release of mineral nutrients and in energy transfer processes. Their diversity and activity may regulate the health and stability of soil ecosystems. Therefore, understanding and utilizing soil bacterial communities is of great potential significance for maintaining ecosystem resilience and promoting sustainable practices on cultivated lands [14]. Soil bacteria represent a key factor in biogeochemical cycles and have become the focus of an increasing volume of researches. These in-depth studies have shed much light on the interpretation of biogeochemical cycles. However, using traditional methods for these researches, almost 99% of soil bacteria cannot be isolated and/or cultured [15]. This large proportion of uncultured soil bacteria ‘dark matter’ [16] greatly limits our understanding of soil functions and processes. In Northeast China, DGGE (denaturing gradient gel electrophoresis) fingerprinting and other traditional biological identification methods have been used to assess microbial biogeographical distributions in black soils [17]; however, these techniques provided ordinary resolution of the communities. In the systematic classification of bacteria, 16S rDNA is the most useful and commonly used molecular clock which is a moderate sized molecule that exists in all organisms, and with high conservation in structure and function. However, the V3~V4 region of 16S rDNA is of high variability, which is usually used for DNA amplification and identification of soil bacterial diversity [17].

In recent years, the rapid development of molecular biology has provided new avenues for soil microbial research; in particular, the development of high-throughput sequencing techniques for 16S rDNA has produced great advancements. These techniques have become widely used in the study of soil microbial ecology and genetics due to their superior accuracy, efficiency, and sensitivity [18–20], even being used to identify novel microbial species and comprehensively survey microbial communities [21,22]. The Illumina MiSeq PE250 has become a mainstream sequencing platform for bacterial 16S rDNA sequencing, due to the advantages of appropriate read length, short sequencing cycles, and high throughput.

Farmland shelterbelts in mid-western Heilongjiang Province are important to ensure national food security. Healthy, stable shelterbelts are critical for promoting stability in local ecosystems. Forest soil microorganisms can also play an important role in maintaining and improving soil fertility and in forest carbon and energy cycles [23,24]. However, the effect of long-term planting of farmland shelter forests on soil fertility remains poorly characterized. Bezemer, et al. [25] undertook a comprehensive review of mechanisms driving bacterial β diversity and phylogenetic β diversity in two temperate forests. However, variation in the soil bacterial communities due to tree species identity was not considered; furthermore, studying functional genes in bacterial communities should corroborate drivers of community changes. In the black soil area of Northeast China, Liu, et al. [26] studied the diversity and distribution of bacterial communities in farmland soils, finding that Acidobacteria was the most common phylum; however, this study did not include shelterbelt soils. To date, few studies exist on soil bacterial communities in shelterbelts using 16S rDNA high-throughput sequencing exist. Therefore, this study used high-throughput sequencing to characterize soil bacterial communities in different shelterbelt types and to predict soil fertility by the functional gene characteristics and their relative abundance. This study could deepen the understanding of the mechanisms that drive farmland shelterbelt soil fertility and provide a theoretical basis for the regulation of soil fertility and quality in farmland shelterbelts.

2. Materials and Methods

2.1. Sample Plot Characteristics and Sample Collection

This study took place in Fengchan Town in Baiquan County, Heilongjiang Province (47°38′4″N–47°39′23″N, 125°18′638″E–125°51′18″E). In this region, the annual frost-free period lasts for 120 to 125 days, with a mean annual temperature of 1.3 °C and an annual effective accumulated

temperature ($\geq 10\text{ }^{\circ}\text{C}$) of $2454.5\text{ }^{\circ}\text{C}$; the mean number of hours of sunshine received annually is 2717.1 h . The average annual precipitation totals 496.7 mm and its seasonal distribution is uneven, where located in the semi-humid zone. In the growing season, the temperature averages $17\text{ }^{\circ}\text{C}$. The annual wind speed averages 3.0 m/s and the wind direction is mostly from the southwest, averaging $202^{\circ}30'$ degrees azimuth. The main crops are corn, soybean, sorghum, and potato. The growing season is from April to September, lasting for about five months. According to the Chinese Soil Classification System, there are five soil types in the region: 67.9% of soils are black soils, 14.4% black calcium soils, 17.1% meadow soils, 0.5% marsh soils and 0.2% salty soils [27], where belongs to high altitudes and cold and dry agricultural areas. The overall soil pH in the study area varied from 6.22 to 8.62 [27].

In this study, the selected five types of farmland shelterbelts and one cropland abandoned for 20 years in this study were all located in the black soil area. The shelterbelts were all well preserved, far from man-made structures (thus subject to little human interference), and their soil conditions before establishing the farmland shelterbelt were basically the same. Each farmland shelterbelt was composed of the following different tree species: “X” contained *Populus xiaohei*, “L” contained *Larix gmelinii* (Rupr.) Kuzen., “Z” contained *Pinus sylvestris* var. *mongholica* Litv., “SL” contained a mix of *Fraxinus mandshurica* Rupr. and *Larix gmelinii* (Rupr.) Kuzen., “ZL” contained a mix of *Pinus sylvestris* var. *mongholica* Litv. and *Larix gmelinii* (Rupr.) Kuzen., and abandoned cropland “CK” severed as a control. All forests were roughly similar in age (20 years old). Three $20\text{ m} \times 8\text{ m}$ sample plots were established in each forest shelterbelt and in the abandoned cropland. Soil samples were collected at five points within each plot, following an “S” shape, on 21 July 2018. After removing the litter layer at each point, two 5 g soil samples were collected: one sample from 0 to 10 cm (the upper soil layer) and another sample from 10 to 20 cm (the lower soil layer) below the surface. Visible impurities, such as rocks and roots, were removed before each sample was passed through a sterile, 2 mm mesh sieve. Samples from all five points in the same layer of a given plot were combined in equal quantities and then stored in sterile centrifuge tubes. Thus, a total of 36 samples were collected and transported to the laboratory on dry ice for later DNA extraction [26]. At the same time, some key survey factors about forest and tree characteristics were also measured. Table 1 describes the basic characteristics of each sample plot.

Table 1. Basic characteristics of the different types of sample plots.

Plot Types	Height /m	DBH /cm	Spacing /m	Longitude and Latitude	Altitude /m
X	17.86 ± 1.77	16.64 ± 2.03	2×1.5	$125^{\circ}51'12.4''\text{E}$ — $125^{\circ}51'38.0''\text{E}$, $47^{\circ}38'22.8''\text{N}$ — $47^{\circ}38'26.2''\text{N}$	241~241
L	9.44 ± 1.55	11.00 ± 2.51	2×1.5	$125^{\circ}48'59.7''\text{E}$ — $125^{\circ}49'03.5''\text{E}$, $47^{\circ}38'38.2''\text{N}$ — $47^{\circ}38'55.3''\text{N}$	239~267
Z	8.18 ± 1.29	12.59 ± 1.67	2×1.5	$125^{\circ}51'37.9''\text{E}$ — $125^{\circ}51'41.4''\text{E}$, $47^{\circ}38'11.9''\text{N}$ — $47^{\circ}38'24.8''\text{N}$	248~251
SL	9.76 ± 1.47	10.99 ± 2.69	2×3	$125^{\circ}49'03.3''\text{E}$ — $125^{\circ}49'06.4''\text{E}$, $47^{\circ}38'23.6''\text{N}$ — $47^{\circ}38'36.8''\text{N}$	242~252
ZL	11.08 ± 1.40	13.96 ± 2.98	2×1.5	$125^{\circ}47'15.5''\text{E}$ — $125^{\circ}47'17.4''\text{E}$, $47^{\circ}39'09.6''\text{N}$ — $47^{\circ}39'30.5''\text{N}$	249~256
CK	—	—	—	$125^{\circ}48'28.1''\text{E}$ — $125^{\circ}48'29.9''\text{E}$, $47^{\circ}38'35.6''\text{N}$ — $47^{\circ}38'36.4''\text{N}$	221~222

Note: X, *Populus xiaohei* farmland shelterbelt; L, *Larix gmelinii* (Rupr.) Kuzen. farmland shelterbelt; Z, *Pinus sylvestris* var. *mongholica* Litv. farmland shelterbelt; SL, *Fraxinus mandshurica* Rupr. mixed with *Larix gmelinii* (Rupr.) Kuzen. farmland shelterbelt; ZL, *Pinus sylvestris* var. *mongholica* Litv. mixed with *Larix gmelinii* (Rupr.) Kuzen. farmland shelterbelt; and CK, abandoned cropland.

2.2. DNA Extraction and PCR Amplification

Total soil DNA was extracted from all 36 samples using an E.Z.N.A.® DNA isolation kit (Omega Bio-Tek Co., LTD, Norcross, GA, USA), according to the manufacturer’s instructions. A NanoDrop ND-1000 ultraviolet spectrophotometer (Thermo Fisher Scientific, Wilmington, MA, USA) was used to

quantify the extracted DNA. All samples were required to have a concentration of at least $20 \text{ ng} \cdot \mu\text{L}^{-1}$, at least 500 ng of DNA, a volume of at least 25 μL and an A260/A280 ratio of between 1.8 and 2.0. The DNA quality was assessed on a 0.8% agarose gel, and samples without obvious RNA bands were retained. The DNA samples that met the above requirements were stored at -20°C prior to further analysis.

The total DNA from each soil sample was used as a template for PCR (polymerase chain reaction) amplification of the highly variable V3~V4 region of the bacterial 16S rDNA. For DNA amplification, the researchers used different primers to obtain different amplicons according to the research purpose, but the primers of the V3~V4 region of bacterial 16S rDNA amplification usually used were standard primers. The forward primer 338F (5'-barcode + ACTCCTACGGGAGGCAGCA-3') and the reverse primer 806R (5'-GGACTACHVGGGTWTCTAAT-3') were used [28]; a 7-bp barcode was included in the forward primer to distinguish among samples in the same library. A thermocycler was used for PCR amplification (Gene Amp 9700, ABI, Foster, CA, USA), with each 25 μL reaction containing 0.25 μL of Q5 High-Fidelity DNA polymerase ($5 \text{ U} \cdot \mu\text{L}^{-1}$), 5 μL of Q5 reaction buffer (5 \times), 5 μL of Q5 High-Fidelity GC Buffer (5 \times), 2 μL (2.5 mM) of dNTPs, 2 μL of the DNA template, 1 μL (10 μM) of the forward and the reverse primer, and 8.75 μL of ddH₂O. Each PCR consisted of an initial denaturation at 98°C for 2 min, followed by 25 cycles of denaturation at 98°C for 15 s, annealing at 55°C for 30 s, and extension at 72°C for 30 s, with a final extension of 5 min at 72°C . Each sample was amplified in triplicate.

PCR amplicons from the same sample were run on a 2% agarose gel to separate fragments by size. Then, target fragments were then cut from the gel and purified using the Axygen DNA gel kit (Axygen Biosciences, Union City, CA, USA), before quantification with a Quant-iT PicoGreen dsDNA Assay Kit (Invitrogen, Carlsbad, CA, USA) and microplate reader (BioTek, FLx800). Samples were combined proportionally into libraries, in accordance with sequencing requirements.

2.3. Library Construction and Illumina Miseq Sequencing

The 250 bp paired-end, 250 bp sequencing libraries were prepared using the TruSeq Nano LT DNA Library Prep Kit (Illumina, San Diego, CA, USA), following the manufacturer's instructions. To check library quality, 1 μL of each library was analyzed on a 2100 Agilent Bioanalyzer instrument using an Agilent High Sensitivity DNA Analysis Kit (Agilent, Santa Clara, CA, USA). Libraries were confirmed to have a single peak with no breaks in the distribution. Libraries were quantified using a Quant-iT PicoGreen dsDNA Assay Kit (Life Technologies, Carlsbad, CA, USA); for sequencing, libraries were required to have a concentration of at least 2 nM. Libraries were sequenced on an Illumina MiSeq PE250 instrument with the MiSeq Reagent Kit V3 (600 cycles). All raw sequences were deposited in the NCBI Sequence Read Archive under accession number SRP187158.

2.4. Data Processing

First, the QIIME (quantitative insights into microbial ecology) pipeline (version 1.8.0, <http://qiime.org/>) was used to conduct quality screening of FASTQ data using the sliding window method. The window size was 10 bp and the step size 1 bp: the first window began at the first base of the 5' end of a sequence. The average base quality score in each window was at least 20 (the average accuracy of base calls was 97%). Sequences were truncated to remove windows with an average quality score lower than Q20; all truncated sequences were at least 150 bp in length, and no ambiguous bases or suspicious sequences were included. Usearch (version 5.2.236, <http://www.drive5.com/usearch/>) was used to search for and remove chimeric sequences [29]. Subsequently, the FLASH software package (version 1.2.7, <http://ccb.jhu.edu/software/FLASH/>) (Magoc and Salzberg, 2011) was used to merge Read 1 and Read 2 in cases that passed preliminary screening. Reads were required to overlap by at least 10 bp and have no mismatched bases. Merged sequences were then assigned to samples using barcodes; in this way, all sequences were collated for each sample.

Secondly, the UCLUST comparison tool of the QIIME [30] was implemented to assign validated sequences into corresponding OTUs according to 97% sequence similarity [31]. The sequences with the highest abundance for each OTU were selected as representative of that OTU. These representative sequences were then BLASTed (basic local alignment search tool) [32] against the Silva database (release 115; <http://www.arb-silva.de>) to obtain taxonomic information; a similarity of 0.999 was considered a match. In order to ensure accuracy, OTUs accounting for less than 0.001% of all sequences were removed [33] and the modified OTU abundance matrix was calculated.

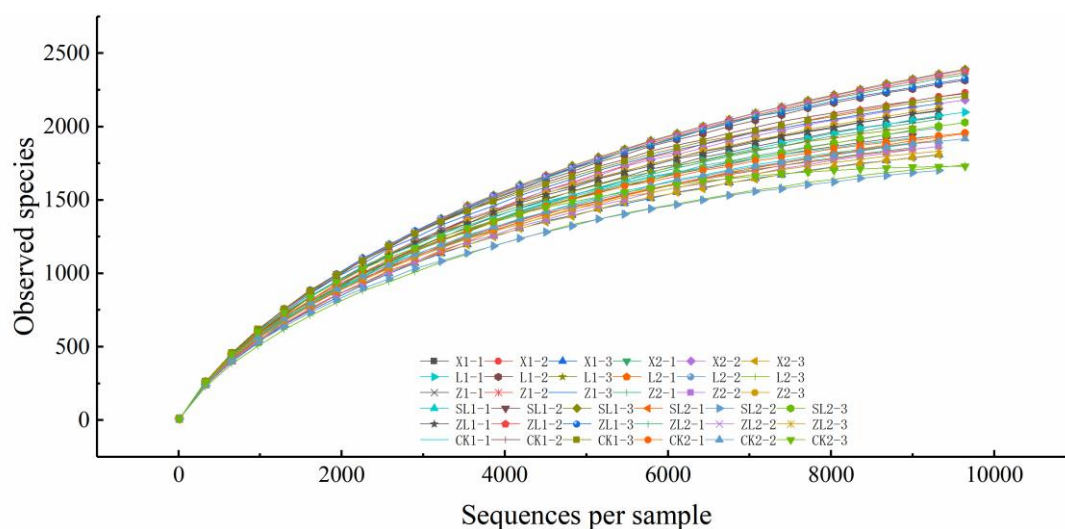
In order to control for effects of sequencing depth on observed OTU diversity, all samples were randomly resampled at the lowest observed sequencing depth level of 90% [34]. QIIME was then used to calculate the ACE (abundance-based coverage estimator), Chao1 richness estimator, Simpson index and Shannon diversity index for each sample or group [26]. For each sample, a statistical table of sample composition at each taxonomic level was created. Differences among samples in species diversity indexes and among the various taxonomic levels were assessed using SPSS 24.0 (IBM, Armonk, NY, USA).

Lastly, the Metastats algorithm [35] in the Mothur software package (<http://metastats.cbcb.umd.edu/>) was used to compare the abundance of observed phyla and genera across study samples; these data were visualized as violin plots. The top 50 genera, based on OTU abundance, were included in cluster analysis and used to create heat maps in R. The distribution of β diversity differences among samples was examined using unweighted NMDS (nonmetric multi-dimensional scaling) with UniFrac distances. A network analysis of the Spearman rank correlations [36] among the 50 most abundant genera was performed using Mothur. All test sequences were compared to the Greengenes 16S rDNA full-length sequence database (<http://greengenes.secondgenome.com/>) using PICRUSt (phylogenetic investigation of communities by reconstruction of unobserved states, developed by Curtis Huttenhower's research group of Harvard University, http://huttenhower.sph.harvard.edu/galaxy/tool_runner?tool_id=PICRUSt_normalize) to find the nearest neighbors of the reference sequences; these were merged for each OTU, using the reference sequence copy number to obtain a corrected OTU abundance matrix. Finally, the bacterial community composition in the corrected matrix was mapped to the KEGG metabolic pathway analysis database (<http://www.genome.jp/kegg/pathway.html>) to annotate and predict metabolic and other potential gene functions in the communities from each sample plot [37]. This study focused on the annotation and prediction of the 12 common functional metabolisms at the second level and the KO (KEGG orthologous groups) metabolic at the fourth level.

3. Results and Analysis

3.1. Sequencing Effectiveness and OTU Statistics for Study Samples

After quality control, a total of 1,418,914 valid sequences were obtained across all 36 samples, with an average of 39,414 sequences per sample. Among these, 99.93% of the sequence reads ranged from 400 bp to 450 bp. After grouping sequences into OTUs, a total of 121,164 OTUs were identified, with 10,687 OTUs remaining after removing rare OTUs, and then 10,184 OTUs remaining after controlling for sequencing depth. Figure 1 depicts the rarefaction curves for all samples. These curves nearly achieve a plateau (beginning with 6000 sequences per sample) and L2–3 reached a stable state, demonstrating that the sequencing depth was adequate to capture the microbial diversity of the samples. The sampling therefore accurately reflected the bacterial communities surveyed and reliably documented their structure.



Note: Different uppercase letters indicate different types of sample plots, the first number following the letter indicates the soil layer ("1" upper and "2" lower); the second number indicates the replicated plot ID.

Figure 1. Rarefaction curves of each soil sample.

Table 2 outlines the OTU distribution for each type of shelterbelt and in each soil layer after controlling for sequencing depth. Considering each type separately, the upper soil layer contained more unique OTUs (i.e., the OTUs that only occur in a single plot type for a given soil layer) than the lower layer; however, across plots, more shared OTUs (i.e., the OTUs that occur across sample types in a given soil layer) were found in the lower versus upper soil layer. This suggests that the upper soil layer supports greater microbial diversity. In both the upper and the lower soil layer, the most unique OTUs were found in CK and the least in SL. Among sites, the coefficient of variation between the upper and the lower soil layers was highest in SL (9.56%) and lowest in L (3.29%), suggesting an especially marked difference between soil layers in SL.

Table 2. Unique OTUs and shared OTUs for each type of soil layer across study sites.

Layer	Unique OTUs						Shared OTUs
	X	L	Z	SL	ZL	CK	
Upper	2519	2374	2368	2299	2455	3410	420
Lower	2268	2266	2093	2008	2268	3234	432
CV (%)	7.72	3.29	8.72	9.56	5.60	3.75	1.99

Note: Unique OTUs only occur in a single plot type for a given soil layer, shared OTUs occur across sample types in the given soil layer.

Table 3 depicts the distribution of OTUs across the six type of study sites, providing both the number of unique and shared OTUs for the upper and the lower soil layers (Here, unique OTUs are those that occur only in a single soil layer of a given sample, whereas shared OTUs are those that occur in both layers). In both X and L, the number of unique OTUs was higher in the lower versus upper soil layer, while the opposite pattern occurred at the other sample sites. A comparing of the upper and the lower soil layer showed that the highest coefficient of variation was seen in SL (25.96%) and the lowest in Z (1.96%). Thus, the vertical distribution of soil microbial diversity varied with forest type, differing most in SL and least in Z. The highest number of shared OTUs was found in ZL and the lowest in X, while the total number of OTUs was greatest in ZL and smallest in CK. Forest soils contained more OTUs than CK soils, with ZL having the highest overall bacterial OTU diversity.

Table 3. Unique OTUs and shared OTUs for upper and lower soil layers across all types of study sites.

Sample		X	L	Z	SL	ZL	CK
Unique OTUs	Upper	1493	1430	1462	1696	1586	977
	Lower	1597	1941	1422	1170	1403	696
Shared OTUs		1847	1893	2016	1887	2342	2282
Total		4937	5264	4900	4753	5331	3955
CV (%)		4.76	21.44	1.96	25.96	8.66	23.75

Note: Unique OTUs occur only in a single soil layer of a given sample, shared OTUs occur in both layers of a given sample.

3.2. Bacterial OTU Alpha Diversity

The Simpson, Chao1, ACE and Shannon alpha diversity indexes are presented in Table 4 for the upper and the lower soil layers of each sample type. In both soil layers, each of the four α diversity indices generally did not differ among sites ($p > 0.05$, i.e., the threshold value set for significance throughout this study, unless otherwise specified), with the exception of the ACE index in the lower soil layer, which differed between CK2 and ZL2 ($p < 0.05$).

Table 4. Diversity indices of soil bacterial communities across all six types of study sites.

Sample	Simpson	Chao1	ACE	Shannon
X1	1.00 ± 0.00a	2415.56 ± 313.95a	2628.13 ± 394.88a	9.62 ± 0.18a
L1	1.00 ± 0.00a	2583.06 ± 264.11a	2814.98 ± 320.18a	9.80 ± 0.28a
Z1	1.00 ± 0.00a	2395.76 ± 190.76a	2573.73 ± 234.52a	9.86 ± 0.19a
SL1	1.00 ± 0.00a	2525.06 ± 433.90a	2741.37 ± 518.70a	9.84 ± 0.23a
ZL1	1.00 ± 0.00a	2884.11 ± 138.48a	3097.92 ± 248.01a	10.02 ± 0.10a
CK1	1.00 ± 0.00a	2495.38 ± 266.87a	2633.57 ± 289.19a	10.06 ± 0.07a
<i>p</i> -value	0.22	0.38	0.50	0.13
X2	1.00 ± 0.00a	2300.21 ± 278.30a	2497.11 ± 306.65ab	9.74 ± 0.16a
L2	1.00 ± 0.00a	2280.97 ± 268.93a	2472.52 ± 310.77ab	9.59 ± 0.28a
Z2	1.00 ± 0.00a	2483.66 ± 168.47a	2702.35 ± 195.05ab	9.75 ± 0.17a
SL2	1.00 ± 0.00a	2382.02 ± 427.27a	2486.05 ± 342.33ab	9.67 ± 0.17a
ZL2	1.00 ± 0.00a	2673.35 ± 518.46a	2947.23 ± 620.24a	9.94 ± 0.21a
CK2	1.00 ± 0.00a	2074.42 ± 297.47a	2187.47 ± 395.47b	9.84 ± 0.07a
<i>p</i> -value	0.51	0.44	0.320	0.31

Note: Different lowercase letters indicate significant differences in pairwise comparisons ($p < 0.05$), the number following each type sample plot ID indicates the soil layer ("1" upper and "2" lower), the values in the table are mean ± S.D., the same as below.

3.3. Bacterial Community Composition

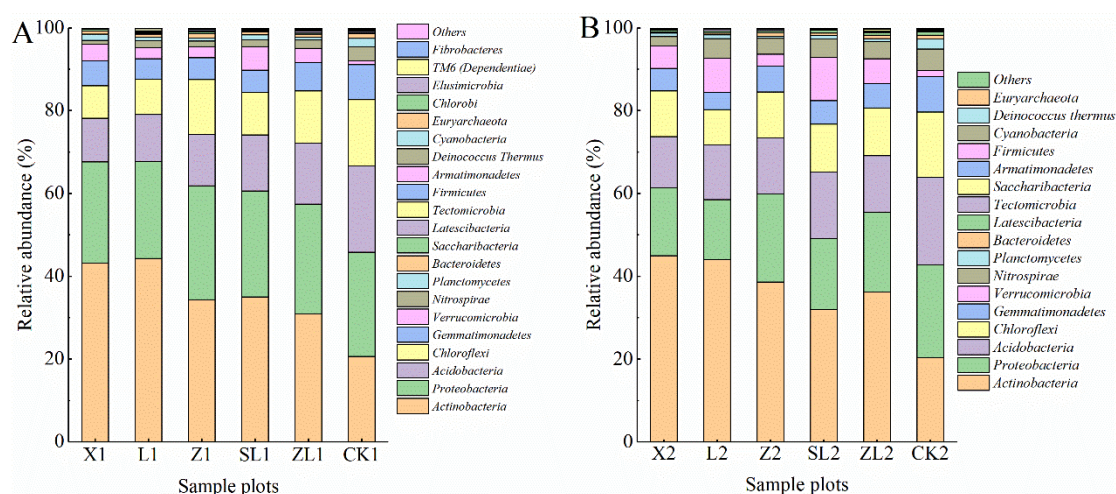
3.3.1. Composition of Soil Bacterial Communities at Each Taxonomic Level

In this study, the total number of phyla, classes, orders, families, genera, and species identified were 27, 86, 97, 189, 303 and 88, respectively. Table 5 shows the classification for each type of study shelterbelt and soil layer. Overall, the mean number of phyla, families, genera, and species did not vary among sites in either the upper or the lower soil layer; however, there were significant differences at the class and order levels. By implementing planned LSD (least significance difference method) ($\alpha = 0.05$) multiple comparisons, differences among sites were identified at most taxonomic levels, with the exception for at the phylum level in the lower soil layer and at the genus level in both soil layers. At the class and order levels, both CK1 and CK2 differed from all other samples within their respective soil layers. At the family level, ZL2 differed from X2. However, there were no statistically significant differences among different forest types at the phyla, genus and species level.

Table 5. Composition of soil bacterial communities at each type of study site by taxonomic level.

Sample	Phylum	Class	Order	Family	Genus	Species
X1	18.33 ± 0.58ab	54.67 ± 2.89c	71.00 ± 6.08b	134.00 ± 6.93b	180.67 ± 13.65	82.67 ± 8.02ab
L1	16.00 ± 2.00b	57.00 ± 2.00bc	76.00 ± 4.36b	145.33 ± 6.35ab	192.33 ± 8.02	90.33 ± 8.08a
Z1	17.33 ± 1.15ab	57.67 ± 4.51bc	73.33 ± 3.21b	142.00 ± 7.00ab	193.33 ± 11.59	86.67 ± 8.33ab
SL1	18.67 ± 2.08ab	60.00 ± 1.73b	73.67 ± 0.58b	142.33 ± 8.51ab	196.33 ± 13.05	83.33 ± 9.07ab
ZL1	17.67 ± 2.08ab	60.33 ± 2.08b	78.67 ± 3.21b	149.33 ± 7.09a	195.33 ± 4.93	89.33 ± 2.52ab
CK1	20.00 ± 1.73a	68.67 ± 2.31a	90.67 ± 4.51a	150.33 ± 5.51a	196.00 ± 5.57	76.33 ± 3.51b
p-value	0.17	0.01	0.01	0.12	0.44	0.23
X2	18.00 ± 1.73	57.00 ± 3.61b	68.33 ± 6.81b	129.00 ± 4.36c	159.33 ± 4.93	76.67 ± 6.51ab
L2	17.33 ± 2.52	58.00 ± 2.00b	69.67 ± 1.53b	130.67 ± 11.15bc	160.33 ± 18.90	72.67 ± 6.66ab
Z2	16.33 ± 0.58	58.00 ± 6.08b	71.67 ± 5.03b	140.67 ± 6.03abc	183.67 ± 18.58	81.00 ± 9.17a
SL2	17.33 ± 1.53	61.67 ± 2.89b	69.67 ± 5.03b	129.67 ± 4.04bc	162.00 ± 10.54	75.33 ± 6.43ab
ZL2	16.67 ± 1.15	62.00 ± 2.00b	74.33 ± 4.73b	145.33 ± 2.89a	179.67 ± 5.51	77.33 ± 6.51ab
CK2	18.67 ± 1.15	68.00 ± 1.73a	87.67 ± 4.73a	143.67 ± 11.37ab	165.67 ± 8.74	65.33 ± 4.62b
p-value	0.51	0.02	0.00	0.05	0.13	0.18

Figure 2 illustrates the relative abundance of observed phyla in the soil bacterial community for each forest type. A total of 22 phyla were identified in the upper soil layer and 18 in the lower. In the upper soil layer (Figure 2A), the five phyla with the highest abundance were the Actinobacteria, Proteobacteria, Acidobacteria, Chloroflexi, and Gemmatimonadetes; here, these dominant phyla accounted for 92.07%, 92.61%, 92.83%, 89.84%, 91.63%, and 91.16% of the total OTU abundance in X1, L1, Z1, SL1, ZL1, and CK1, respectively. Actinobacteria were more abundant in forest soils (minimum relative abundance of 30.99% in ZL1, maximum relative abundance of 43.25% in X1) than in CK (where relative abundance was 20.66%), while the Acidobacteria and Gemmatimonadetes were more abundant in CK (relative abundance of 20.82%, 8.48%, respectively) than in the forest soils (the maximum relative abundance recorded was 14.74% and 6.82%, respectively). In the lower soil layer (Figure 2B), the four most abundant phyla were the Actinobacteria, Proteobacteria, Acidobacteria, and Chloroflexi; these phyla accounted for 84.78%, 80.33%, 84.59%, 76.79%, 80.66%, and 79.72% of the total in X2, L2, Z2, SL2, ZL2, and CK2, respectively. Again, the Actinobacteria were more abundant in the forest (minimum relative abundance was 32.05% in ZL2, maximum relative abundance of 45.01% in X2) versus CK (20.43%) soils, while the other three dominant phyla were more common in CK (relative abundance of 22.38%, 21.05%, and 8.50%, respectively) than in the shelterbelts (the maximum relative abundance was 21.27%, 16.19%, and 6.23%, respectively).



Note: The number following the sample plot ID indicates the upper ("1") or lower ("2") soil layer, i.e., (A) denotes the upper soil layer, (B) denotes the lower soil layer (the meanings of A and B in the figure are the same in the following figures).

Figure 2. The relative abundance of bacterial communities at the phylum level.

Figure 3. Heat maps comparing bacterial community composition at the genus level for the six types of study sites.

In the upper soil layer (Figure 3A), SL1, L1, Z1, and ZL1 were similar in terms of their microbial composition. In X1, species of *Asanoa*, *Dactylosporangium*, *Luedemannella*, and *Micromonospora* were highly abundant (1.84%, 2.26%, 0.89%, and 1.09%, respectively), while in L1, *Solirubrobacter* and *Streptomyces* were most common (0.74%, and 1.81%, respectively). In Z1, the most abundant genera were *Acidothermus*, *Blastococcus*, *Nocardioides*, and *Nordella* (0.39%, 0.56%, 0.36%, and 0.46%, respectively), while in SL1, highly abundant genera included 11–24, *Lapillicoccus* and *Ochrobactrum* (0.37%, 0.44%, and 0.61%, respectively); and in ZL1, the most common genera included CL500–29 marine group, *Pseudolabrys* and *Sphingomonas* (0.81%, 0.35%, and 3.80%, respectively). Finally, in CK1 the most common genera were *Bryobacter* and *Ilumatobacter* (0.88%, and 0.88%, respectively). In the lower soil layer (Figure 3B), X2 was similar to Z2 in terms of microbial composition, while L2 was similar to SL2 and ZL2. The most common genus in X2 was *Roseiflexus* (relative abundance of 1.63%). In L2, *Acidothermus*, *Candidatus Xiphihymenobacter* and *Nocardioides* were most common (2.55%, 0.74%, and 0.78%, respectively), while *Blastococcus*, *Mesorhizobium*, *Ochrobactrum*, *Sediminibacterium* and *Variibacter* were most common in Z2 (0.22%, 0.47%, 1.41%, 0.38%, and 1.44%, respectively). Meanwhile, RB41 dominated in SL2 (4.41%), while *Kribbella* and *Phenylobacterium* were abundant in ZL2 (0.80%, and 0.23%, respectively). Finally, in CK2, the most abundant genera were *Asanoa*, *Haliangium*, *Iamia*, and *Ilumatobacter* (1.66%, 1.62%, 0.43%, and 0.53%, respectively). There were more dominant genera in the upper soil layer than in the lower soil layer. Genera that were highly abundant in both layers included *Acidothermus*, *Nocardioides*, *Blastococcus*, *Ochrobactrum*, *Asanoa*, and *Ilumatobacter*. In both soil layers, these genera were most common in Z.

3.3.2. Differences in Taxonomic Composition Among Study Sites

Figure 4 provides boxplots of the abundance (in terms of OTUs) of both in the upper soil layer (Figure 4A) and in the lower soil layer (Figure 4B) across the six types of study sites at the phyla level; these phyla showed the greatest variation among sites were selected according to pairwise comparison tests ($p < 0.05$). As can be seen from Figure 4A, there were 12 phyla that varied significantly in abundance among the study sites, and these accounted for 44.44% of all phyla. Among these phyla, those with the highest abundance were the Acidobacteria, Actinobacteria, Chloroflexi, Gemmatimonadetes, and Verrucomicrobia. Acidobacteria, Armatimonadetes, Chloroflexi, Gemmatimonadetes, Latescibacteria, Nitrospirae, and Planctomycetes were more abundant in CK1 than in the forest samples. In Figure 4B, there were 13 phyla that varied significantly in abundance among the study sites; these phyla accounted for 48.12% of the total phyla. Among these phyla, those with the highest abundance were the Acidobacteria, Actinobacteria, Gemmatimonadetes, Nitrospirae, Proteobacteria, and Verrucomicrobia. Acidobacteria, Armatimonadetes, Gemmatimonadetes, Latescibacteria, Nitrospirae, Planctomycetes, and Proteobacteria were more abundant in CK2 than in the forest samples. A comparison of data in Figure 4A,B shows that the Chlorobi, Chloroflexi, and Euryarchaeota all varied significantly among study sites in the upper soil layer, but not in the lower soil layer. Meanwhile, Bacteroidetes and Cyanobacteria showed the reverse pattern. A comparison of the different forest types indicates that the Actinobacteria showed the greatest differences in abundance.

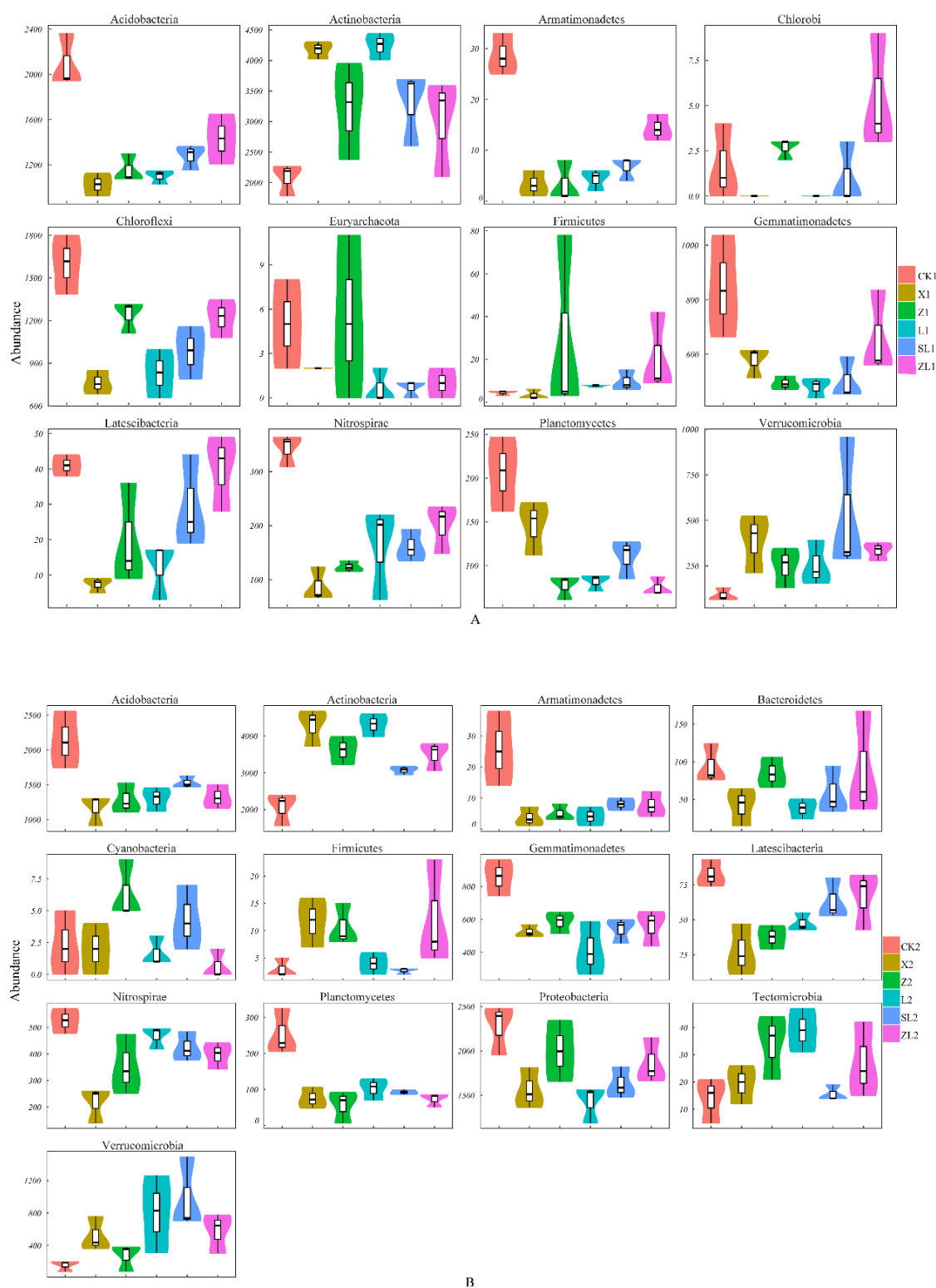


Figure 4. Boxplots of abundance for phyla and genera with significant differences at the phyla level.

Figure 5 provides boxplots of the abundance (in terms of OTUs) of both in the upper soil layer (Figure 5A) and in the lower soil layer (Figure 5B) across the six types of study sites at the genus level; these genera showed the greatest variation among sites and were selected according to pairwise comparison tests ($p < 0.05$). As can be seen from Figure 5A, there were 20 genera that varied significantly among sites. Among these genera, those with the highest abundance were *Actinoplanes*,

Asanoa, *Dactylosporangium*, *Haliangium*, and *Jatrophihabitans*, and these differences were driven by relatively high abundance in CK1 or X1. Similarly, as shown in Figure 5B, there were also 20 genera that varied significantly among the study sites. Among these genera, those with the highest abundance were *Candidatus Solibacter*, *Krasilnikovia*, *Microclunatus*, and *Nitrobacter*, which all had high abundance in forest samples. A comparison of Figure 5A,B shows that *Novosphingobium* and *Planosporangium* varied significantly across the study sites in both soil layers. A comparison of the different forest types shows that *Actinoplanes* differed most in the upper soil layer and *Krasilnikovia* in the lower soil layer.

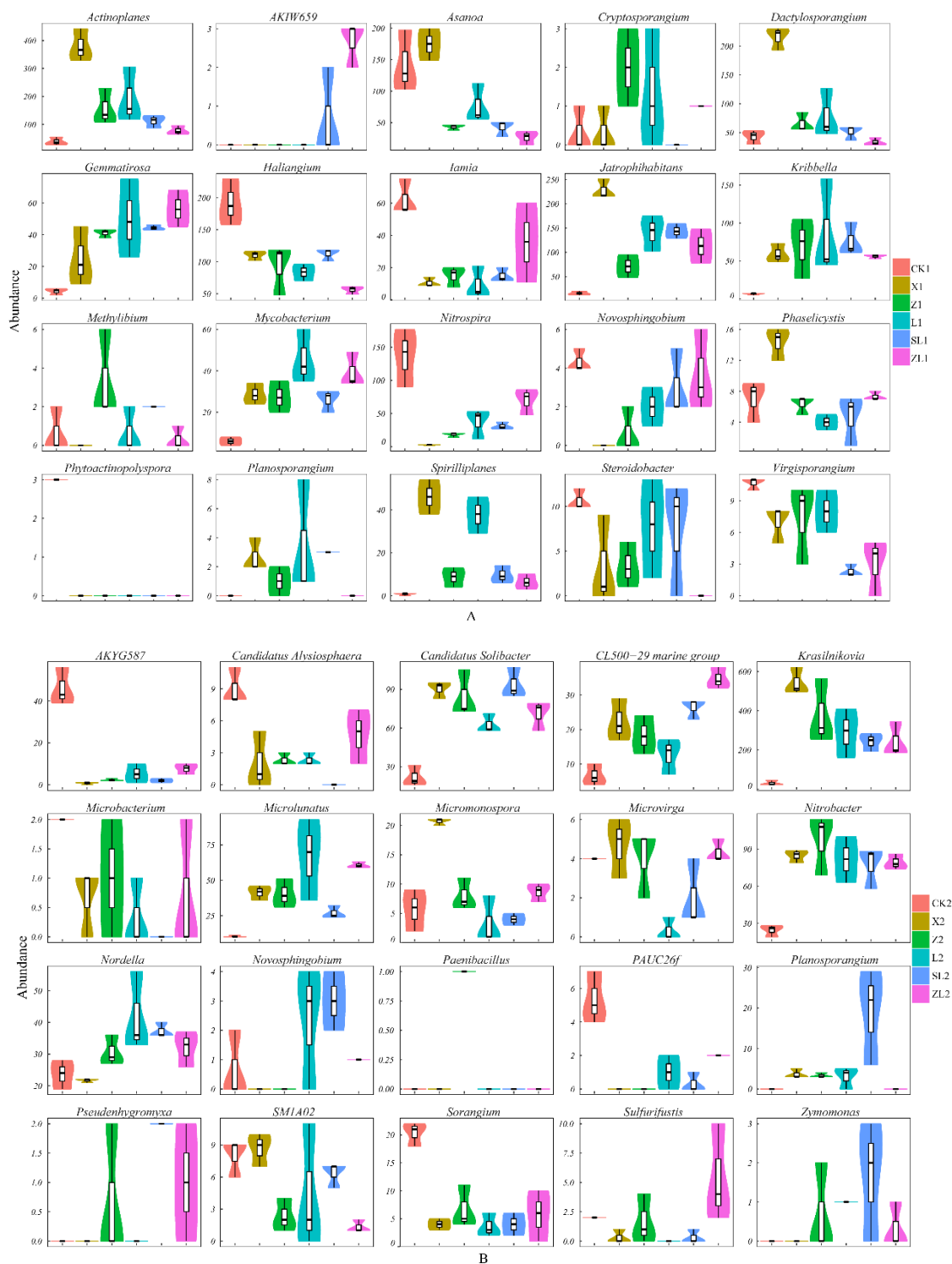


Figure 5. Boxplots of abundance for phyla or genera with significant differences at the genus level.

3.4. Bacterial OTU Beta Diversity

Beta diversity reflects similarities in community structure among different groups of samples. UniFrac is a distance metric that reflects phylogenetic relationships among unique OTUs in a community, thus more comprehensively revealing similarities among community samples. Figure 6 shows the first two axes of an NMDS based on unweighted UniFrac distances (Figure 6A,B indicates the upper soil layer and the lower soil layer, respectively). The community structure of the CK samples differed significantly from that of the forest samples, and there was also a large difference among the L samples. However, the community structure of L1 was similar to Z1, SL1, and ZL1, while SL2 was similar to Z2 and ZL2.

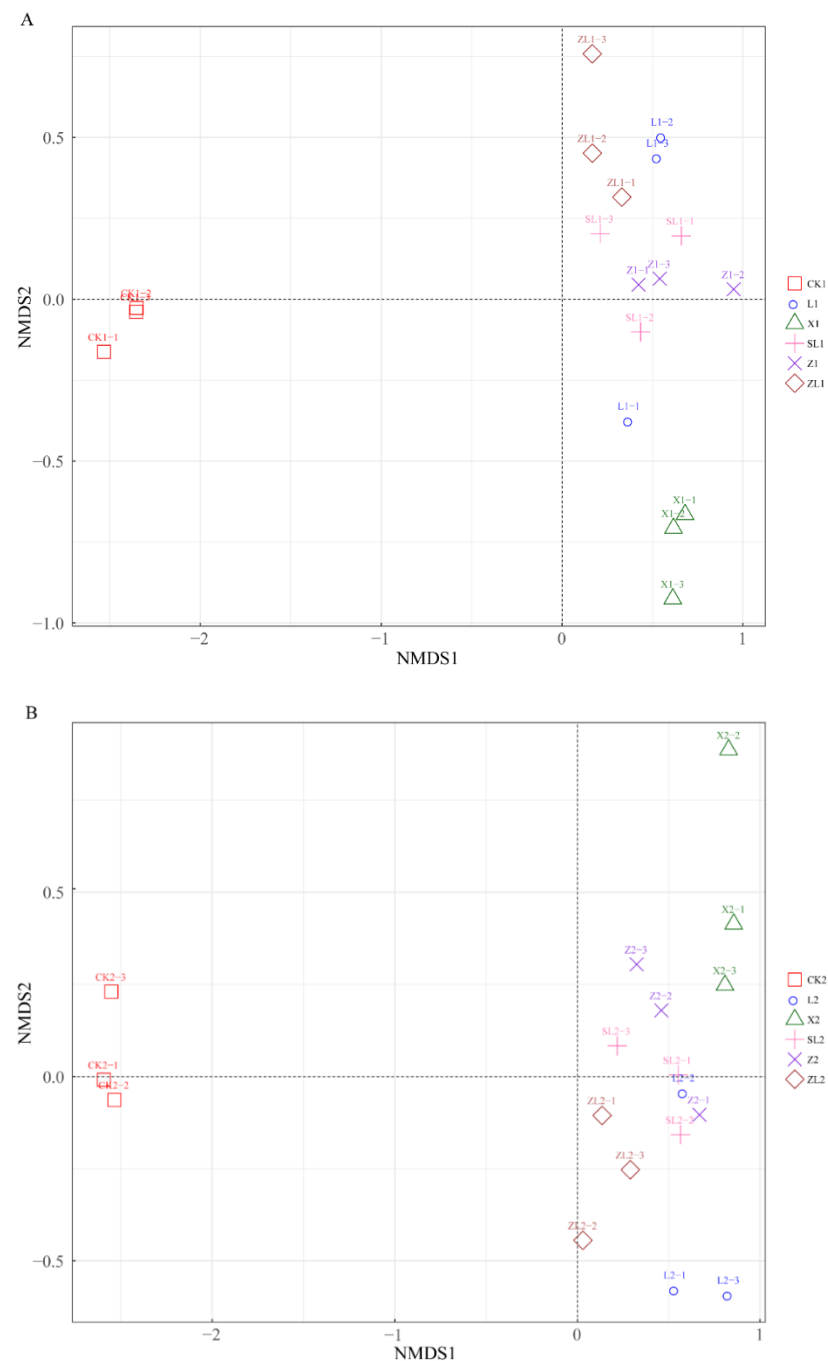
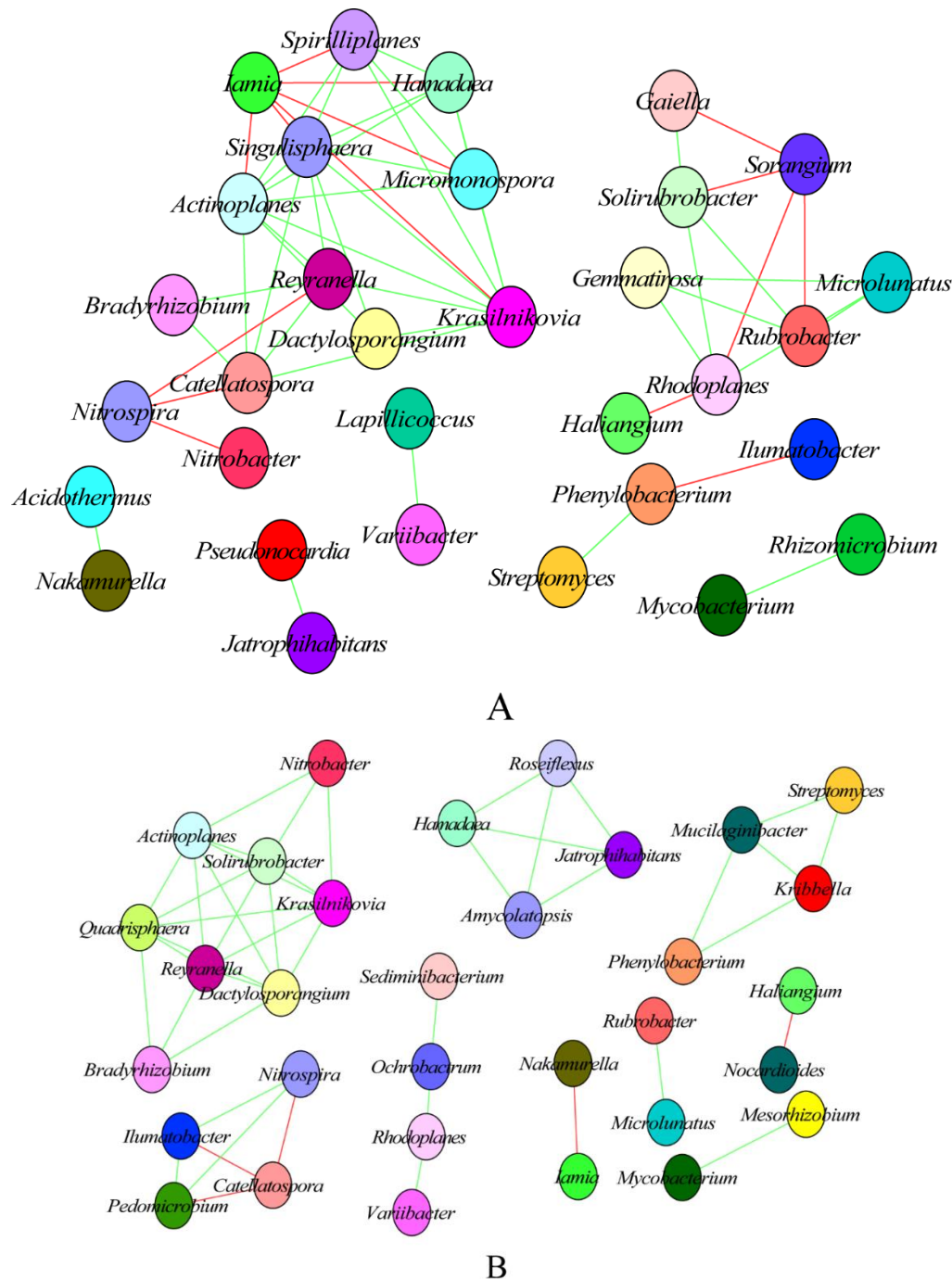


Figure 6. NMDS 2D sorting diagram of the sample plots based on unweighted UniFrac distances.

3.5. Network Analysis of Associations Among Genera

To investigate interactions among genera within communities, Spearman's rank-order correlation coefficients were calculated among the 50 most abundant genera and a correlation network diagram was constructed for all such dominant genera with $|rho| > 0.6$ and $p < 0.01$ (Figure 7).



Note: The node is the name of the genus, the line indicates a correlation between the two genera, the green line is a positive correlation, the red line is a negative correlation, the number of the connecting line of one node reflects the degree of correlation with other genera.

Figure 7. Association network diagrams of dominant genera.

The association network for the 30 dominant genera in the upper soil layer is found in Figure 7A. Relationships among genera can be divided into the following three categories: lone pair correlations, chain correlations, and network correlations. The relationships between *Lapillicoccus* and *Variibacter*, *Pseudonocardia* and *Jatrophihabitans*, and *Rhizomicrobium* and *Mycobacterium* represent positive, lone-pair correlations. Considering chain correlations, *Phenylobacterium* was positively correlated with *Streptomyces* but negatively related to *Ilumatobacter*. Considering network correlations, *Iamia* was negatively correlated with *Krasilnikovia*, *Actinoplanes*, *Micromonospora*, *Hamadaea*, *Spirilliplane*, and *Singulisphaera*; whereas *Nitrospira* was negatively correlated with *Catellatospora*, *Nitrobacter*, and *Reyranella*; and *Sorangium* was negatively correlated with *Rubrobacter*, *Rhodoplanes*, *Solirubrobacter*, and *Gaiella*. *Actinoplanes*, *Krasilnikovia*, and *Singulisphaera* all had the largest number of nodes and were positively correlated with each other; these three genera were also all positively correlated with *Catellatospora*, *Dactylosporangium*, *Hamadaea*, *Micromonospora*, *Reyranella*, and *Spirilliplanes*.

The association network for the 28 genera found in the lower soil layer is shown in Figure 7B. The relationships between *Microtholunatus* and *Rubrobacter*, *Mycobacterium* and *Mesorhizobium* represent positive lone-pair correlations, while those between *Nocardioideis* and *Haliangium* as well as *Iamia* and *Nakamurella* represent negative lone-pair correlations. The genera *Sediminibacterium*, *Ochrobactrum*, *Rhodoplanes*, and *Variibacter* formed a positive chain correlation. Considering network correlations, *Actinoplanes*, *Dactylosporangium*, *Krasilnikovia*, *Quadrisphaera*, *Reyranella*, and *Solirubrobacter* were all positively correlated, multi-associated genera with six nodes each. *Amycolatopsis*, *Hamadaea*, *Jatrophihabitans*, and *Roseiflexus* all had positive pair-wise correlations.

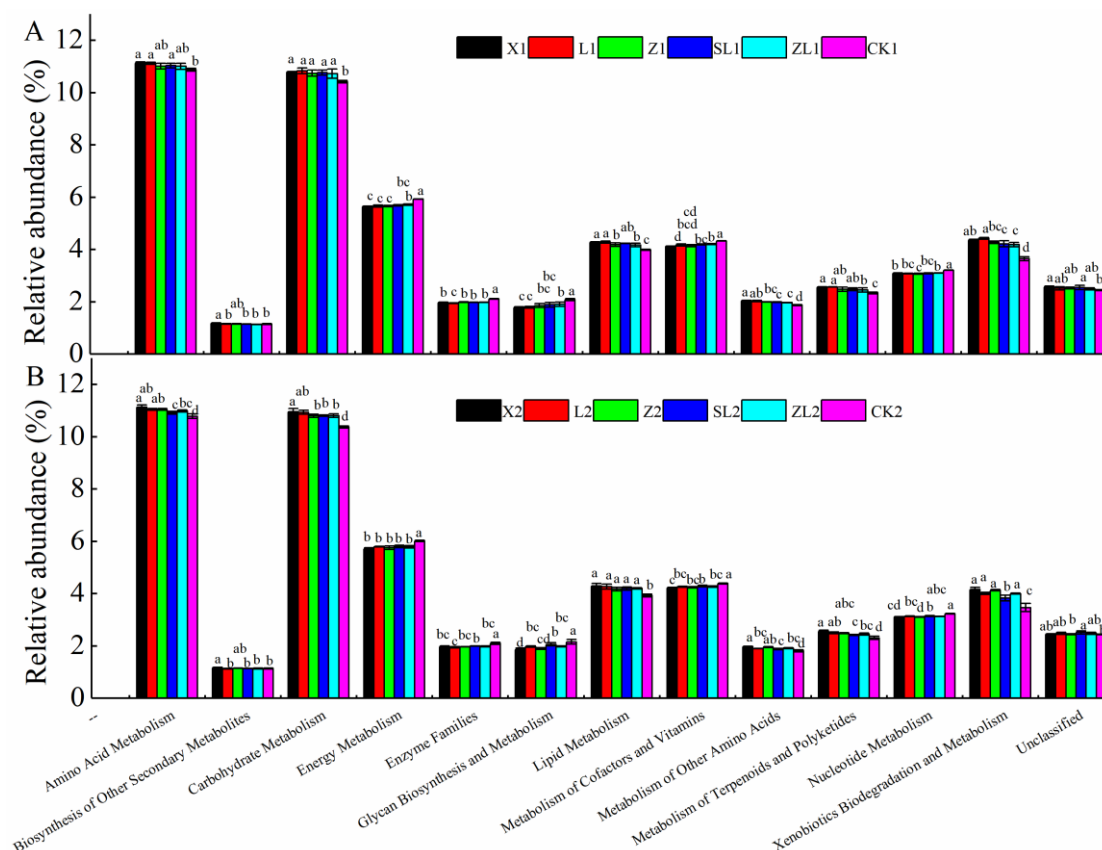
Comparing the upper and the lower soil layers, *Actinoplanes* and *Krasilnikovia* were the two genera with the highest number of associations, suggesting that they play important roles in the construction of microbial communities. *Nitrospira*, *Iamia*, and *Sorangium* were negatively correlated with other genera in the upper soil layer, but not in the lower soil layer. Bacterial networks of competition and cooperation were more complex among genera in the upper than in the lower soil layer.

3.6. Microbial Community Function

3.6.1. Microbial Metabolism

Figure 8 presents the metabolic predictions by PICRUSt for the bacterial communities from each type of study site created using the KEGG database at level 2. The abundance of the 12 metabolites was basically the same in the upper (Figure 8A) and lower soil layers (Figure 8B). Amino acid and carbohydrate metabolism functions were highly represented, suggesting these play a dominant role in total community metabolism. In contrast, the biosynthesis of other secondary metabolites was relatively weak, suggesting it play a weaker role in total metabolism.

The functional categories of nucleotide metabolism, metabolism of cofactors and vitamins, glycan biosynthesis and metabolism, energy metabolism and enzyme families each accounted for a higher percentage of the total in CK than in the forest samples. However, the carbohydrate metabolism, lipid metabolism, metabolism of other amino acids, and metabolism of terpenoids and polyketides categories showed the reverse pattern. A sizeable proportion of unclassified metabolites (about 3.00%) was also found. Comparing shelterbelt types, there was no difference in the proportions of functional genes involved in amino acid or carbohydrate metabolism in the upper soil layer. In the lower soil layer, energy metabolism and lipid metabolism genes were equally represented. Functional genes involved in amino acid metabolism were less abundant in the upper soil layer of SL versus the other forest types.



Note: Different lowercase letters indicate significant differences in pairwise comparisons ($p < 0.05$), the same as the below.

Figure 8. Prediction of the abundance of functional metabolic gene contents.

3.6.2. Functional Potential of Bacterial Homologous Gene Clusters

The potential metabolic functional capabilities of each sample were predicted based on KO (KEGG orthology) IDs retrieved from the database, as well as the relative abundance of enzymes involved in nutrient cycling according to the KEGG metabolic pathway database (at the 4th hierarchy level). The gene relative abundances referred to carbon, nitrogen, sulfur, and phosphorus cycles were measured.

The results for carbon cycle enzymes are presented in Figure 9, which divides the enzymes into four categories. Seven functional gene clusters were identified from the samples as follows: two type of carbon fixation enzymes, 1, 5-bisphosphate ribulose carboxylase/oxygenase (*rbcL*, EC:4.1.1.39, K 01601 and *rbcS*, EC:4.1.1.39, K01602); two type of cellulolytic enzymes, endoglucanase (EC:3.2.1.4, K01179) and β -glucuronidase (*uidA*, EC: 3.2.1.31, K01195); two type of xylanolytic enzymes, endo-1,4- β -xylanase (*xynA*, E3.2.1.8, K01181) and xylan 1,4- β -xylosidase (*xynB*, EC:3.2.1.37, K01198); and a type of lignin decomposing enzyme, catechol 1, 2-dioxygenase (*catA*, EC:1.13.11.1, K03381). In the upper soil layer (Figure 9A), the relative abundance of the carbon fixation enzyme K01601 varied among shelterbelt types, while K01602 did not. The relative abundance of the cellulolytic enzyme K01179 was significantly higher in CK (0.1113%) than in the shelterbelts. The relative abundance of the xylanolytic enzymes K01181 and K01198 did not vary among shelterbelts. The highest relative abundance of lignin lyases occurred in L (0.0136%). In the lower soil layer (Figure 9B), the carbon fixation enzyme K01601 had the highest relative abundance in SL (0.0084%). The cellulolytic enzyme K01179 and xylanolytic enzyme K01181 were most common in SL (0.1024%, 0.0664%) and least common in ZL (0.0027%, 0.0283%). The lignin decomposing enzyme K03381 was the least relative abundant in ZL (0.0063%). Both carbon fixation enzymes and lignin decomposing enzymes were more common

in the upper than in the lower soil layer. The cellulose decomposition enzyme K01179 and xylanase K01181 accounted for the largest proportion of the total enzyme pool across samples. The relative abundance of cellulose decomposition enzymes and xylanolytic enzymes was higher in the lower versus upper soil layer. Hence, the carbon fixation capacity of the upper soil layer was stronger than that of the lower soil layer. Also, the potential for organic matter decomposition was greatest in SL, weakest in ZL, and intermediate in L, X, and Z (which did not differ from one another).

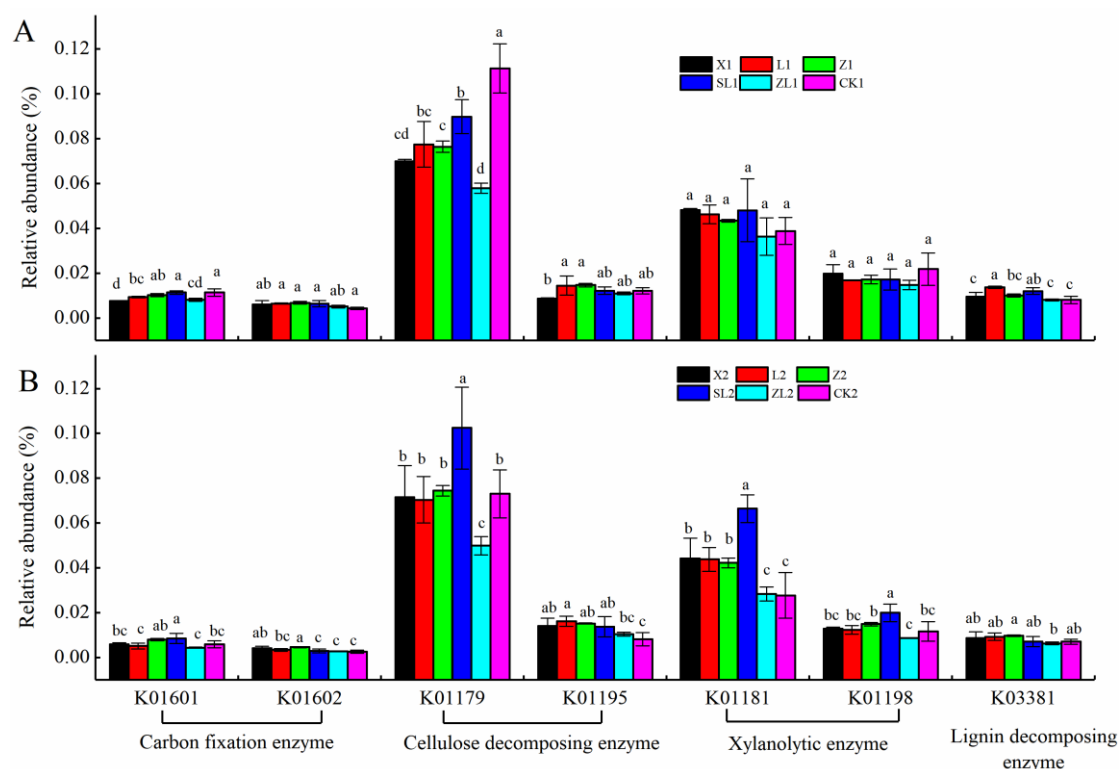


Figure 9. Relative abundance distribution histogram of enzymes reflecting the carbon cycle.

The results for nitrogen cycle enzymes, which were divided into three functional categories, are presented in Figure 10. Identified enzymes included a nitrogenase iron protein (*NifH*, EC:1.18.6.1, K02588), a copper-containing nitrite reductase involved in denitrification (*nirK*, EC:1.7.2.1, K00368) and a nitrite reductase containing a cytochrome C-552 subunit (*nrfA*, EC:1.7.2.2, K03385) involved in dissimilatory nitrate reduction to ammonium (DNRA). In the upper soil layer (Figure 10A), the relative abundance of the nitrogenase K02588 was highest in CK (where it was significantly higher than in forest soils) and lowest in ZL (0.0126%). A comparison of shelterbelts shows that the nitrite reductase K00368 was most abundant in SL (0.0128%) and least abundant in X (0.0061%), while the relative abundance of the nitrate dissimilation reductase K03385 did not vary with forest type. In the lower soil layer (Figure 10B), the relative abundance of the nitrogenase K02588 was highest in CK (0.0231%) and SL (0.0195%) (not significantly different from each other) and lowest in ZL (0.0101%). The relative abundance of the nitrite reductase K00368 was also highest in SL (0.0189%), but the lowest in CK (0.0055%). Lastly, the relative abundance of the nitrate dissimilation reductase K03385 was significantly higher in SL (0.0131%) than in the other types. A comparison of the upper and the lower soil layers shows that the nitrate dissimilation reductase K03385 was at higher levels in the lower soil layer. The relative abundance of nitrate reductase K00368 was significantly higher in SL than in other shelterbelts. Thus, CK soils had a greater capacity for nitrogen fixation than the forest soils; nitrite and nitrate reduction potential was highest in SL and weakest in X.

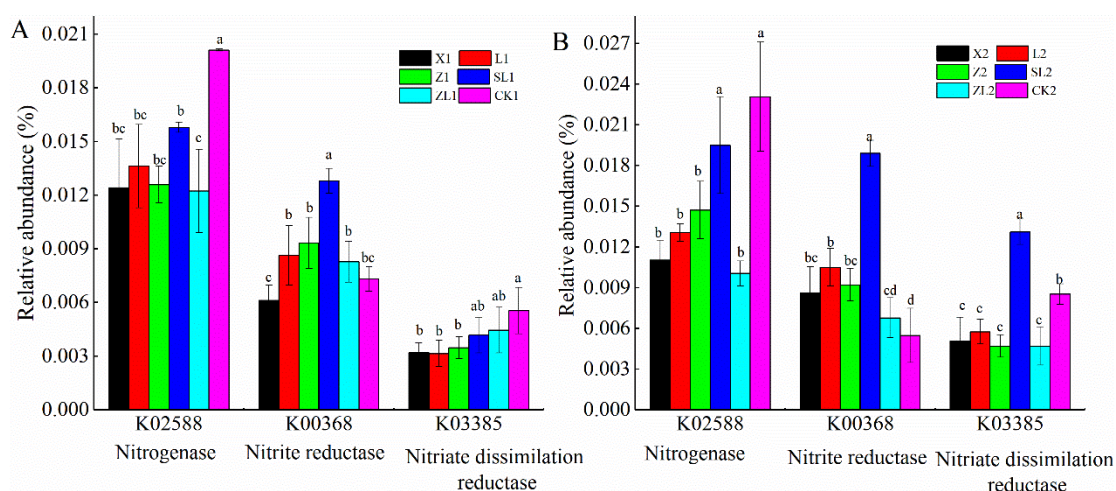


Figure 10. Relative abundance distribution histogram of enzymes reflecting the nitrogen cycle.

Five functional gene clusters, grouped into the following two categories, were identified for phosphorus cycling (Figure 11): Category one, three type of acidic phosphatases, acidic phosphatase 4-phytase (*appA*, EC:3.1.3.26, K01093), acid phosphatase-A (*phoN*, EC:3.1.3.2, K09474) and PHO (*pho*, EC:3.1.3.2, K01078) and category two, two type of alkaline phosphatases, alkaline phosphatase (EC:3.1.3.1, K01077) and alkaline phosphatase-D (*phoD*, EC:3.1.4.1, K01113). In the upper soil layer (Figure 11A), the relative abundance of the acidic phosphatase K09474 was lower in the forest versus CK soils (0.0076%), while the acidic phosphatase K01078 was most relative abundant in SL (0.0325%). The relative abundance of the alkaline phosphatase K01077 was lowest in X (0.0111%), while the alkaline phosphatase-D K01113 was most common in CK (0.0674%) and SL (0.0608%) (not different from one another). In the lower soil layer (Figure 11B), the relative abundance of the acidic phosphatases, K01093 and K01078, was highest in SL (0.0124%, 0.0325%), while the relative abundance of K09474 was highest in CK (0.0080%). The relative abundance of the alkaline phosphatase K01077 was significantly higher in SL (0.0334%) than in the other forest types but did not differ from CK (0.0220%). The relative abundance of the alkaline phosphatase-D K01113 was lowest in ZL (0.0315%). A comparison of the upper and the lower soil layers shows that K01093 and K01113 were present at higher proportions in the upper soil layer. In general, phosphatase relative abundance was advantageous in CK and SL, but inhibitory in X and ZL. Alkaline phosphatase activity was higher than that of the acidic phosphatases in all samples.

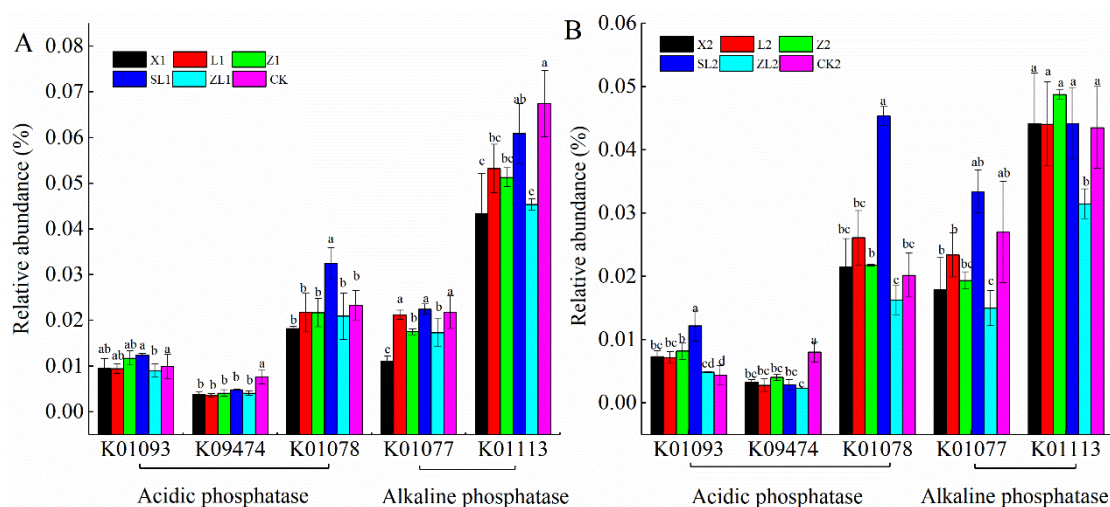


Figure 11. Relative abundance distribution histogram of enzymes reflecting the phosphorus cycle.

Enzyme relative abundances involved in the sulfur cycle were illustrated in Figure 12. Identified enzymes included two type of sulfate assimilation reductases, phosphoadenosine phosphosulfate reductase (*cysH*, EC:1.8.4.8, K00390) and adenylylsulfate kinase (*cysC*, EC:2.7.1.25, K00860), and two type of sulfate dissimilating reductases, adenylylsulfate reductase subunit A (*aprA*, EC:1.8.99.2, K00394) and adenylylsulfate reductase subunit B (*aprB*, EC:1.8.99.2, K00395). In the upper soil layer (Figure 12A), the relative abundance of the sulfate assimilation reductase K00390 was highest in SL (0.0599%). Furthermore, the relative abundance of the sulfate assimilation reductase K00860 in Z (0.0266%) differed from the other study sites, while both K00394 and K00395 were higher in CK (0.0127%, 0.0047%, respectively) than in forest soils. In the lower soil layer (Figure 12B), sulfate assimilating reductase K00390 was least abundant in ZL (0.0323%), while sulfate assimilating reductase K00860 was most abundant in SL (0.0522%). The relative abundance of the sulfate dissimilating reductase K00394 did not vary with forest type but was lower in forest soils than in CK soil samples. Finally, the sulfate dissimilating reductase K00395 was most abundant in SL (0.0070%). A comparison of the upper and the lower soil layers shows that the sulfate dissimilating reductases were relatively more abundant in the lower soil layer. In general, the sulfate assimilating reductases were more abundant than the sulfate dissimilating reductases. Assimilating reductases were most dominant in SL and least in ZL, while dissimilating reductases were more dominant in CK and least in X.

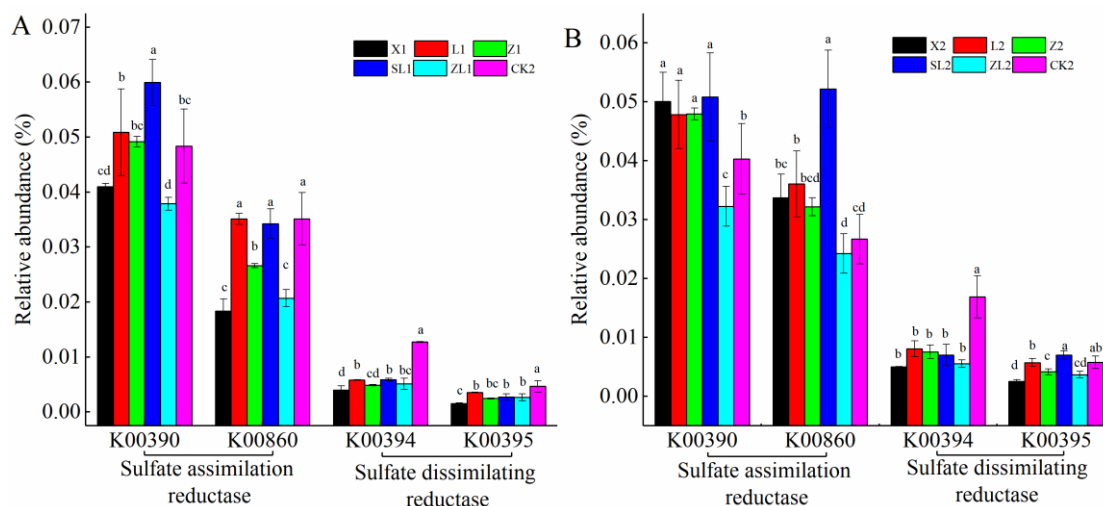


Figure 12. Relative abundance distribution histogram of enzymes reflecting the sulfur cycle.

4. Discussion

4.1. Diversity of Soil Bacterial Communities in Shelterbelts of Different Forest Types

This study is the first to use high-throughput sequencing technology to characterize soil bacterial communities in shelterbelt forests in midwestern Heilongjiang Province, China. Previous studies [38–40] have shown that the distribution of microorganisms can be influenced by environmental heterogeneity and dispersal limitation, but these effects vary with the microbial domain, habitat type, spatial scale, and taxonomic level [41]. The microbial diversity of woodland soils may be directly related to the vegetation cover, soil and land use type [42]. In this study, the average number of sequences obtained per shelterbelt sample (39,414) was much higher than that reported for arable land (13,685) [43]; indicating greater soil bacterial community diversity in farmland shelterbelts versus arable lands in Chinese black soils. With increasing sequencing depth, the number of OTUs should continue to increase, so black soil microbial communities have more OTUs than other soil types. A comparison of the bacterial diversity among forests composed of different tree species shows that the number of unique OTUs was highest in CK. However, a comparison of the upper soil layer with the lower soil layer shows that the number of unique and total OTUs was lowest in CK and the number of total OTUs was highest in ZL. Thus, there

were more shared OTUs among the forest types. This finding of variation in the number of unique OTUs among forest types was consistent with that of Yang, et al. [44] and Niu, et al. [45]. However, Carnovale, et al. [46] considered that shelterbelt systems which contain a mixture of different plant genera have the potential to exhibit greater microbial community heterogeneity than single-species plantations. These differences may be due to different vegetation above the soil. The ACE diversity index was higher in ZL than CK in the lower soil layer; thus, the lower soil layers in ZL were more supportive of bacterial diversity than those of CK. A comparison with the research results of [28] shows that the changes of bacterial diversity index of X and Z in our research results were different, which may be related to the different forest types and specific tree species: our plots were belt forest, while theirs were sheet forest; the poplar we selected for the test is *Populus × xiaohei*, while theirs was *Populus × canadensis* Moench.

Liu, et al. [43] documented that Acidobacteria is widespread and common in the soil. However, Actinobacteria were the most dominant phylum in the soils of the five forest types tested here, consistent with the findings of Niu, et al. [45], but different from those of Li, et al. [47] and Deng, et al. [28], who found that the Acidobacteria were most common. This inconsistency may be related to soil pH, as the *Larix gmelinii* forest soils in Li, et al. [47] were acidic, while the soils in this study were neutral or slightly alkaline. Preem, et al. [48] also considered soil pH as a key factor in shaping bacterial community structures. However, the abundance of Acidobacteria was higher in Z than that in X, which was consistent with Lauber, et al. [49] who found the relative abundance of Acidobacteria was relatively higher in the coniferous forest than those of broadleaf forest. A study of soil bacteria in cherry forests [50] found the Proteobacteria to be dominant, also inconsistent with this study, perhaps due to differences in litter content. Finally, another study also failed to find a high abundance of Actinobacteria [51], perhaps due to varying humidity levels. As the previous findings [52,53] had established that both tree species and afforestation time dramatically influenced soil characteristics, then the changes in soil properties alter habitats, resulting in different microbial communities. The dominant phyla found here (e.g., Actinobacteria, Proteobacteria, Acidobacteria, Chloroflexi, Gemmatimonadetes, Planctomycetes, and Bacteroidetes) were the same as those found by Liu, et al. [26], and were also consistent with descriptions of microbial communities from 88 soils collected in North and South America [54] and 29 soils collected in the Arctic [38]; however, the order of dominant phyla (in terms of abundance) differed among studies, perhaps due to the different PCR primers used and different vegetation composition among sites. Navarrete, et al. [55] found that the relative abundance of Acidobacteria decreased significantly with the transformation of Amazon forest soils to agricultural soils, which were consistent with the results in our study (soil Acidobacteria were more common in the abandoned agricultural land than in shelterbelts). The abundance of Proteobacteria in X was higher than that in Z, which was inconsistent with Deng, et al. [28]. The reason may be the forest ages of X and Z were inconsistent in Deng's study. Gemmatimonadetes were another dominant bacterial community in our research, similar to a study by DeBruyn, et al. [56] study, who found Gemmatimonadetes in arid soils, such as grassland, prairie, pasture, pine trees soil, were higher abundance. Thus, in this study, we believed that the differences in soil dominant bacterial genera among forest shelterbelts were due to variation in habitat.

A recent β diversity analysis revealed differences in the soil microbial flora among forest types [57]. In this study, comparing study sites, the composition of microbial communities at the genus level in forest samples differed from CK; however, SL, ZL, and L had similar soil bacterial communities, perhaps as all three shelterbelts contained *Larix gmelinii*. These findings were consistent with the findings of Ren, et al. [58] and Gunina, et al. [59], and also verify the hypothesis of Deng, et al. [28] about the influence of tree species on soil bacterial communities. Meanwhile, this study confirms the hypothesis of Bezemer, et al. [25] that soil bacteria would show strong intraspecific aggregation, according to different environmental factors. However, some studies have found that plant species identity had no significant effect on bacterial beta diversity or phylogeny-based β diversity [25,60,61]; this could be due to differences in study variables, such as the PCR primers used, sequencing method,

the variable region amplified, and how the diversity metrics were calculated. For example, the primers used by Bezemer, et al. [25] were 27F and 534R, and the V1~V3 region of the 16S rDNA was amplified. Many researchers have argued that the identity of plant species within a community, as well as factors such as community composition, can distinctly affect microorganism diversity and drive variation in soil nutrients [60,62].

A network analysis of the most abundant genera in the study samples revealed that *Actinoplanes* and *Krasilnikovia* had the most connections to other genera. In all the sample plots, the abundance of these two genera varied the most, and their abundance was generally high, indicating a key role for these genera in the soil bacterial communities of the shelterbelts. In this study, *Actinoplanes* was the dominant genus in the soil bacterial communities of the farmland shelterbelts. Li, et al. [63] also found that *Actinoplanes* was one of the six dominant genera in soil bacterial communities in Sichuan Province. The three genera *Iamia*, *Nitrospira*, and *Sorangium* outcompeted other genera in surface soils, but not in the lower layer soil, suggesting that these genera were represented by aerobic bacteria that performed better closer to the surface. According to the previous studies, *Nitrospira* can oxidize nitrites into nitrates, and this nitrification process is aerobic [64,65], confirming the current analysis of the characteristics of *Nitrospira*.

Soil microbial metabolism is a complicated and changeable process. Among the twelve categories of metabolic processes identified here, most differed among study sites, and these differences were more complex in the upper soil layer. This phenomenon may be related to large differences observed in the surface soil quality across study sites. Surface soils in SL had less litter, more roots, and more loose soil, resulting in faster organic matter decomposition, while surface soils in Z, ZL, and L had more litter cover, harder soils, and fewer roots. Regarding metabolic diversity, the categories of nucleotide metabolism, the metabolism of cofactors and vitamins, glycan biosynthesis and metabolism, energy metabolism, and enzyme families were more abundant in CK than the shelterbelts. However, Castaneda and Barbosa [66] found that the metabolism of amino acids, fatty acids, and nucleotides, as well as genes involved in secondary metabolism, were enriched in forest soils. Thus, habitat characteristics can affect the metabolic function of microbial communities, in contravention of the microbial distribution hypothesis of “random placement” [67]. Among the twelve metabolic categories studied here, amino acid and carbohydrate degradation/metabolism accounted for the greatest proportion [68]. The category of amino acid metabolism was underrepresented in SL, perhaps due to the strong capacity for nitrogen fixation and efficient nitrogen utilization at this site. It also shows that the composition of the dominant forest community in the restored agricultural landscape can change the plant-soil interaction, thus changing the ecological function. This finding is consistent with Carnovale, et al. [46], who studied the relationship between different tree species (*Acacia*, *Eucalyptus*) and soil microbial community structure of the shelterbelts in southeast Australia. The prediction of bacterial metabolic functions is typically limited to the most abundant metabolic pathways and there is also limited information in the KEGG database for bacteria involved in metabolism. In fact, many metabolic functions remain unknown and undocumented in the KEGG database. In addition, there are some metabolites with low abundance but play an important role in micro-ecosystems. All these metabolic functions require further study.

4.2. Function Potential of Soil Bacterial Community in Shelterbelts of Different Forest Types

Gelaw, et al. [69] found that different land use in the semi-arid watershed have obvious effects on soil carbon and nitrogen contents. Carnovale, et al. [46] considered that tree species may alter the rate of fundamental soil processes, such as nutrient cycling and carbon dynamics, through differences in plant microbial associations, amount and quality of leaf and root litter, and root exudates. Gunina, et al. [59] also considered that forest soil properties were altered by the processes of tree establishment, growth, and mortality. Afforestation could improve soil quality, but this effect varied with tree age and species [52]. In this study, the functional potential of soil bacterial communities in different forest shelterbelt was predicted according to the functional gene abundance of soil bacteria involving carbon, nitrogen, phosphorus, and sulfur.

The soil carbon pool is the largest carbon pool in terrestrial ecosystems, including both organic and inorganic carbon. Yan, et al. [70] noted that agricultural soils have a large potential for carbon sequestration. Since inorganic carbon mainly exists in the form of carbonate and has little exchange capacity in the carbon cycle, research on carbon inputs and utilization has mainly focused on carbon fixation enzymes, and the decomposition and new synthesis of organic carbon. Carbon fixation enzymes [71], cellulose decomposing enzymes, polysaccharide decomposing enzymes, and lignin decomposing enzymes [72] are often used as indicators of soil carbon conversion [73]. In this study, the carbon fixation capacity of the upper soil layer was stronger than that of the lower layer, likely a consequence of enhanced microbial activity in the upper layer along with the accumulation of dead branches and leaves. A positive correlation between the carbon sequestration potential of carbon fixation enzymes and soil carbon components has been reported [71,74], also explaining this pattern. The high abundance of lignin decomposing enzymes in the upper soil layer of L may be due to copious amounts of surface litter at this site. The capacity for organic matter decomposition and soil carbon utilization differed among forest types, being highest in SL, followed by the single-species forests and lastly ZL. The coniferous and broad-leaved mixed forest was the most suitable for the survival of bacteria with carbon fixation genes or decomposition genes, both conducive to soil carbon fixation and recycling. This was also found by Lu, et al. [75], who reported differences in soil organic matter content beneath different tree species.

Nitrogen, inorganic nitrogen compounds, and organic nitrogen compounds are the three forms of nitrogen that can be taken up nature. Ninety-five percent of nitrogen in the soil exists as organic nitrogen, which must be first transformed into inorganic nitrogen by microorganisms before it is available to plants [76]. Soil nitrogen fixation, nitrification, denitrification, and ammonification are mainly mediated by soil bacteria [77]. To some extent, the denitrifying community of bacteria plays a vital role in the soil nitrogen cycle, and the relative abundances of specific OTUs are more valuable in predicting community function [78]. In this study, the nitrogenase abundance was higher in CK versus forest soils, and the lowest overall in ZL, a site with loose soils. This could be related to the presence of many leguminous herbs in CK. Nitrogen inputs for forest growth are mainly in the form of nitrate or ammonium salts [79]. DNRA is also an important part of the nitrogen cycle, but it is different from the denitrification of nitrate (denitrification has long been considered a major mechanism of N loss) [80]. The abundance of *NifHs*, *Cu-NiRs*, and *cd1NiRs* were highest in SL, followed by L and Z, and lastly ZL and X; this indicates that SL soils had a good nitrogen supply while X soils had a nitrogen shortage. This result was similar to those of Ma, et al. [81] who studied nitrogen deficiencies in continuously planted poplar forests. This was also consistent with Lu, et al. [75] who found that the total nitrogen content was the highest in *Fraxinus mandshurica* forests, followed by *Larix gmelinii* and *Pinus sylvestris* forests, and lastly poplar forests.

Phosphorus is an indispensable nutrient for biological growth and development. It plays an essential role in energy transmission, signal transmission, macromolecular synthesis, plant photosynthesis, and respiration, among other functions. However, only 20% of the phosphorus available in soils can be directly absorbed and utilized by plants [82]. Phosphate solubilizing microorganisms (PSMs) in the soil can decompose organic phosphorus into inorganic phosphorus which can be absorbed and utilized by plants, and this process depends on the activity of phosphatase [83]. Phosphatases are important enzymes that stimulate activity in soil phosphorus pools. In this study, alkaline phosphatases were more abundant than acidic phosphatases, likely as a result of the pH neutral or alkaline soils in the study area. The abundance of phosphatase genes was higher in SL than the other forest types, suggesting that SL soils were conducive to the activation of soil phosphorus, while ZL soils were mostly unfavorable for phosphorus activation. Phosphorus activation did not differ between the three single-species forests, X, L, and Z, consistent with Lu, et al. [75]. However, in other studies of poplar forests, soil phosphorus content did vary among forest types [81,84]. As the poplar forest soils were low in organic phosphorus, perhaps phosphatase activity was not stimulated, explaining the difference. Wu, et al. [85] linked a decrease in soil phosphorus content in poplar shelterbelts in

black soil area to change in annual mean temperature. However, Ma, et al. [81] hypothesized that differences in phosphatase activity under different tree species could be linked to the phenolic acid content of root secretions; the abundance of phosphatase genes was negatively correlated with the phenolic acid content.

Sulfur is another essential element for plant growth and development, involved in photosynthesis, respiration, nitrogen fixation, protein, and lipid synthesis and other important physiological and biochemical processes. It can enhance tolerance to environmental stress, transport toxic and harmful substances to vacuoles, and protect cells directly from toxicity [86]. Sulfates can synthesize cysteine under the action of assimilating reductases (*cysC* and *cysH*) that convert inorganic sulfur to organic sulfur [87]. In this study, the abundance of sulfate assimilating reductases (*cysC* and *cysH*) was much higher than that of sulfate dissimilating reductases, especially in forest soils, indicating that forest soils had a strong sulfur assimilation effect. Meanwhile, the abundance of sulfate dissimilating reductases (*aprA* and *aprB*) was higher in CK than in forest soils, again suggesting that forest soils were more conducive to sulfur assimilation. The reason for this difference could be poorer soil aeration in CK, meaning that lower soil layers experienced anaerobic conditions and hence were prone to dissimilating reduction reactions [88], consistent with previous research results [86]. The abundance of sulfate assimilating reductases in the different forest types mirrored the abundance of carbon, cellulose, and lignin decomposing enzymes (highest in SL and lowest in ZL), suggesting synergism between the soil carbon and sulfur cycles.

On the basis of the above analysis, we believe that shelterbelt systems containing coniferous broad-leaved mixed tree species could have a greater potential of microbial community function versus coniferous mixed forest or single-species plantations [46]. In terms of soil bacterial function, the abundances of functional genes related to C, N, P, and S in broad-leaved forests were different than that in coniferous forests, which were consistent with the finding of Nair and Ngouajio [89]. Different plantation tree species could distinctly affect the community compositions of decomposers [90], different plantation forests affected soil characteristics [91], thereby causing the change in the soil microbial diversity and functional diversity [28].

4.3. Suggestions for Future Research

In general, there are many factors that influence the microbial diversity of shelterbelt soils, including the distance between sampling points and trees, the sampling, and so on. In this study, sites contained different tree species, but planting density and pre-planting site conditions were similar; also, the fertility potential of forest soils was inferred by the corresponding functional genes. Further studies should focus on other factors, and consider interactions among tree growth, soil physical and chemical properties, and soil microbial communities.

5. Conclusions

(1) The soil bacterial communities varied among forest types. The dominant phyla were Actinomycetes, Proteobacteria, Acidobacteria, Chlorobacteria, and Blastomycetes. The dominant genera were most abundant in Z. The number of unique bacterial OTUs in the upper soil layer was higher than in the lower soil layer and higher in CK than in the shelterbelts. The total number of OTUs was greatest in ZL.

(2) On the basis of a comparison of the shelterbelt forest types, at the phylum level, Actinomycetes showed the greatest variation in abundance among sites. At the genus level, the greatest variation in abundance occurred in the *Actinoplanes* in the upper soil layer, and in *Krasilnikovia* in the lower soil layer.

(3) Relationships among genera were more complex in the upper soil layer and the competition was more intense here than in the lower soil layer. *Actinoplanes* and *Krasilnikovia* were key bacterial genera forming community networks.

(4) In terms of functions such as carbon fixation, organic matter decomposition and assimilation, nitrogen fixation and assimilation, phosphorus solubility, and sulfate assimilation and dissimilation capability, variability was seen among forest types. The soil fertility potential was strongest in SL, followed by Z and L, and lastly ZL and X.

Author Contributions: J.Z. conceived the ideas and designed the study; Y.X. and Y.Z. supervised the design of experiments; J.Z. and Y.X. performed the experiments data collection and analysis; J.Z. wrote the first draft of the manuscript; Y.X. and Y.Z. led the writing.

Funding: This research was funded by the Forestry Industry Research Special Funds for Public Welfare Projects (Grant No. 2014040202-01).

Acknowledgments: The sequencing service was provided by Personal Biotechnology Co., Ltd. Shanghai, China. We thank the anonymous reviewers and the editor for their valuable comments.

Conflicts of Interest: The authors declare no conflict of interest.

References

1. Sun, L.B.; Chang, X.M.; Yu, X.X.; Jia, G.D.; Chen, L.H.; Liu, Z.Q.; Zhu, X.H. Precipitation and soil water thresholds associated with drought-induced mortality of farmland shelter forests in a semi-arid area. *Agric. Ecosyst. Environ.* **2019**, *284*, 106595. [[CrossRef](#)]
2. Edwards, J.; Johnson, C.; Santos-Medellin, C.; Lurie, E.; Podishetty, N.K.; Bhatnagar, S.; Eisen, J.A.; Sundaresan, V. Structure, variation, and assembly of the root-associated microbiomes of rice. *Proc. Natl. Acad. Sci. USA* **2015**, *112*, E911–E920. [[CrossRef](#)] [[PubMed](#)]
3. Hacquard, S.; Schadt, C.W. Towards a holistic understanding of the beneficial interactions across the *Populus* microbiome. *New Phytol.* **2015**, *205*, 1424–1430. [[CrossRef](#)] [[PubMed](#)]
4. Lau, J.A.; Lennon, J.T. Rapid responses of soil microorganisms improve plant fitness in novel environments. *Proc. Natl. Acad. Sci. USA* **2012**, *109*, 14058–14062. [[CrossRef](#)] [[PubMed](#)]
5. Zolla, G.; Badri, D.V.; Bakker, M.G.; Manter, D.K.; Viyanco, J.M. Soil microbiomes vary in their ability to confer drought tolerance to Arabidopsis. *Appl. Soil Ecol.* **2013**, *68*, 1–9. [[CrossRef](#)]
6. Yergeau, E.; Bell, T.H.; Champagne, J.; Maynard, C.; Tardif, S.; Tremblay, J.; Greer, C.W. Transplanting soil microbiomes leads to lasting effects on willow growth, but not on the rhizosphere microbiome. *Front. Microbiol.* **2015**, *6*, 1436. [[CrossRef](#)]
7. Wagner, M.R.; Lundberg, D.S.; Coleman Derr, D.; Tringe, S.G.; Dangl, J.L.; Mitchell Olds, T. Natural soil microbes alter flowering phenology and the intensity of selection on flowering time in a wild Arabidopsis relative. *Ecol. Lett.* **2015**, *18*, 218–220. [[CrossRef](#)]
8. Bennett, A.E.; Grussu, D.; Kam, J.; Caul, S.; Halpin, C. Plant lignin content altered by soil microbial community. *New Phytol.* **2015**, *206*, 166–174. [[CrossRef](#)]
9. Qin, Y.; Pan, X.Y.; Jin, W.; Chen, L.Q.; Yuan, Z.L. Comparison of four extraction methods of soil microbiome in poplar plantation. *Sci. Silvae Sin.* **2018**, *54*, 169–176. [[CrossRef](#)]
10. Rodrigues, R.C.; Araujo, R.A.; Costa, C.S.; Lima, A.J.T.; Oliveira, M.E.; Cutrim, J.A.A.; Santos, F.N.S.; Araujo, J.S.; Santos, V.M.; Araujo, A.S.F. Soil microbial biomass in an agroforestry system of Northeast Brazil. *Trop. Grassl. Forrajes Trop.* **2015**, *3*, 41–48. [[CrossRef](#)]
11. Bulgarelli, D.; Schlaeppi, K.; Spaepen, S.; van Themaat, E.V.L.; Schulze-Lefert, P. Structure and functions of the bacterial microbiota of plants. *Annu. Rev. Plant Biol.* **2013**, *64*, 807–838. [[CrossRef](#)] [[PubMed](#)]
12. Schlaeppi, K.; Bulgarelli, D. The plant microbiome at work. *Mol. Plant Microbe Interact.* **2015**, *28*, 212–217. [[CrossRef](#)] [[PubMed](#)]
13. Shanmugam, S.G.; Magbanua, Z.V.; Williams, M.A.; Jangid, K.; Whitman, W.B.; Peterson, D.G.; Kingery, W.L. Erratum to: Bacterial diversity patterns differ in soils developing in sub-tropical and cool-temperate ecosystems. *Microb. Ecol.* **2017**, *73*, 556–569. [[CrossRef](#)] [[PubMed](#)]
14. Cookson, W.R.; Murphy, D.V.; Roper, M.M. Characterizing the relationships between soil organic matter components and microbial function and composition along a tillage disturbance gradient. *Soil Biol. Biochem.* **2008**, *40*, 763–777. [[CrossRef](#)]
15. Pace, N.R. A molecular view of microbial diversity and the biosphere. *Science* **1997**, *276*, 734–740. [[CrossRef](#)]
16. Jansson, J.K.; Prosser, J.I. Microbiology: The life beneath our feet. *Nature* **2013**, *494*, 40–41. [[CrossRef](#)]

17. Mi, L.; Wang, G.H.; Jin, J.; Sui, Y.Y.; Liu, J.D.; Liu, X.B. Comparison of microbial community structures in four Black soils along. *Can. J. Soil Sci.* **2012**, *92*, 543–549. [[CrossRef](#)]
18. Barriuso, J.; Marin, S.; Mellado, R.P. Effect of the herbicide glyphosate on glyphosate-tolerant maize rhizobacterial communities: A comparison with pre-emergency applied herbicide consisting of a combination of acetochlor and terbuthylazine. *Environ. Microbiol.* **2010**, *12*, 1021–1030. [[CrossRef](#)]
19. Qin, J.J.; Li, R.Q.; Raes, J.; Arumugam, M.; Burgdorf, K.S.; Manichanh, C.; Nielsen, T.; Pons, N.; Levenez, F.; Yamada, T.; et al. A human gut microbial gene catalogue established by metagenomic sequencing. *Nature* **2010**, *464*, 59–67. [[CrossRef](#)]
20. Singh, A.K.; Dubey, S.K. Current trends in Bt crops and their fate on associated microbial community dynamics: A review. *Protoplasma* **2016**, *253*, 663–681. [[CrossRef](#)]
21. Caporaso, J.G.; Lauber, C.L.; Walters, W.A.; Berg-Lyons, D.; Lozupone, C.A.; Turnbaugh, P.J.; Fierer, N.; Knight, R. Global patterns of 16S rRNA diversity at a depth of millions of sequences per sample. *Proc. Natl. Acad. Sci. USA* **2011**, *108*, 4516–4522. [[CrossRef](#)] [[PubMed](#)]
22. Sogin, M.L.; Morrison, H.G.; Huber, J.A.; Mark Welch, D.; Huse, S.M.; Neal, P.R.; Arrieta, J.M.; Herndl, G.J. Microbial diversity in the deep sea and the underexplored “rare biosphere”. *Proc. Natl. Acad. Sci. USA* **2006**, *103*, 12115–12120. [[CrossRef](#)] [[PubMed](#)]
23. Breulmann, M.; Schulz, E.; Weissshuhn, K.; Buscot, F. Impact of the plant community composition on labile soil organic carbon, soil microbial activity and community structure in semi-natural grassland ecosystems of different productivity. *Plant Soil* **2012**, *352*, 253–265. [[CrossRef](#)]
24. Fang, X.M.; Yu, D.P.; Zhou, W.M.; Zhou, L.; Dai, L.M. The effects of forest type on soil microbial activity in Changbai Mountain, Northeast China. *Ann. Forest Sci.* **2016**, *73*, 473–482. [[CrossRef](#)]
25. Bezemer, T.M.; Wang, X.G.; Li, H.; Hao, Z.Q. Drivers of bacterial beta diversity in two temperate forests. *Ecol. Res.* **2016**, *31*, 57–64. [[CrossRef](#)]
26. Liu, J.J.; Sui, Y.Y.; Yu, Z.H.; Yao, Q.; Shi, Y.; Chu, H.Y.; Jin, J.; Liu, X.B.; Wang, G.H. Diversity and distribution patterns of Acidobacterial communities in the black soil zone of northeast China. *Soil Biol. Biochem.* **2016**, *95*, 212–222. [[CrossRef](#)]
27. Sun, J.X.; Zhao, Y.S.; Xin, Y. Soil nutrient changes of different stage of *poplar* farmland shelterbelts in black soil region. *J. Northeast For. Univ.* **2018**, *46*, 13. [[CrossRef](#)]
28. Deng, J.J.; Zhang, Y.; Yin, Y.; Zhu, X.; Zhu, W.X.; Zhou, Y.B. Comparison of soil bacterial community and functional characteristics following afforestation in the semi-arid areas. *PeerJ* **2019**, *7*, e7141. [[CrossRef](#)]
29. Caporaso, J.G.; Kuczynski, J.; Stombaugh, J.; Bittinger, K.; Bushman, F.D.; Costello, E.K.; Fierer, N.; Pena, A.G.; Goodrich, J.K.; Gordon, J.I.; et al. QIIME allows analysis of high-throughput community sequencing data. *Nat. Methods* **2010**, *7*, 335–336. [[CrossRef](#)]
30. Edgar, R.C. Search and clustering orders of magnitude faster than BLAST. *Bioinformatics* **2010**, *26*, 2460–2461. [[CrossRef](#)]
31. Blaxter, M.; Mann, J.; Chapman, T.; Thomas, F.; Whitton, C.; Floyd, R.; Abebe, E. Defining operational taxonomic units using DNA barcode data. *Philos. Trans. R. Soc. B* **2005**, *360*, 1935–1943. [[CrossRef](#)] [[PubMed](#)]
32. Quast, C.; Pruesse, E.; Yilmaz, P.; Gerken, J.; Schweer, T.; Yarza, P.; Peplies, J.; Glockner, F.O. The SILVA ribosomal RNA gene database project: Improved data processing and web-based tools. *Nucleic Acids Res.* **2012**, *41*, D590–D596. [[CrossRef](#)] [[PubMed](#)]
33. Bokulich, N.A.; Subramanian, S.; Faith, J.J.; Gevers, D.; Gordon, J.I.; Knight, R.; Mills, D.A.; Caporaso, J.G. Quality-filtering vastly improves diversity estimates from Illumina amplicon sequencing. *Nat. Methods* **2013**, *10*, 57–59. [[CrossRef](#)] [[PubMed](#)]
34. Buffington, S.A.; Di Prisco, G.V.; Auchtung, T.A.; Ajami, N.J.; Petrosino, J.F.; Costa-Mattioli, M. Microbial reconstitution reverses maternal diet-induced social and synaptic deficits in offspring. *Cell* **2016**, *165*, 1762–1775. [[CrossRef](#)]
35. White, J.R.; Nagarajan, N.; Pop, M. Statistical methods for detecting differentially abundant features in clinical metagenomic samples. *PLoS Comput. Biol.* **2009**, *5*, e1000352. [[CrossRef](#)]
36. Shannon, P.; Markiel, A.; Ozier, O.; Baliga, N.S.; Wang, J.T.; Ramage, D.; Amin, N.; Schwikowski, B.; Ideker, T. Cytoscape: A software environment for integrated models of biomolecular interaction networks. *Genome Res.* **2003**, *13*, 2498–2504. [[CrossRef](#)]

37. Langille, M.G.I.; Zaneveld, J.; Caporaso, J.G.; McDonald, D.; Knights, D.; Reyes, J.A.; Clemente, J.C.; Burkepile, D.E.; Thurber, R.L.V.; Knight, R.; et al. Predictive functional profiling of microbial communities using 16S rRNA marker gene sequences. *Nat. Biotechnol.* **2013**, *31*, 814–821. [\[CrossRef\]](#)
38. Chu, H.Y.; Fierer, N.; Lauber, C.L.; Caporaso, J.G.; Knight, R.; Grogan, P.; Lauber, C.L.; Grogan, P. Soil bacterial diversity in the Arctic is not fundamentally different from that found in other biomes. *Environ. Microbiol.* **2010**, *12*, 2998–3006. [\[CrossRef\]](#)
39. Finlay, B.J. Global Dispersal of Free-Living Microbial Eukaryote Species. *Science* **2002**, *296*, 1061–1063. [\[CrossRef\]](#)
40. Griffiths, R.I.; Thomson, B.C.; James, P.; Bell, T.; Bailey, M.; Whiteley, A.S. The bacterial biogeography of British soils. *Environ. Microbiol.* **2011**, *13*, 1642–1654. [\[CrossRef\]](#)
41. Hanson, C.A.; Fuhrman, J.A.; Horner-Devine, M.C.; Martiny, J.B.H. Beyond biogeographic patterns: Processes shaping the microbial landscape. *Nat. Rev. Microbiol.* **2012**, *10*, 497–506. [\[CrossRef\]](#) [\[PubMed\]](#)
42. Yao, H.; He, Z.; Wilson, M.J.; Campbell, C.D. Microbial Biomass and Community Structure in a Sequence of Soils with Increasing Fertility and Changing Land Use. *Microb. Ecol.* **2000**, *40*, 223–237. [\[CrossRef\]](#) [\[PubMed\]](#)
43. Liu, J.J.; Sui, Y.Y.; Yu, Z.H.; Shi, Y.; Chu, H.Y.; Jin, J.; Liu, X.B.; Wang, G.H. High throughput sequencing analysis of biogeographical distribution of bacterial communities in the black soils of northeast China. *Soil Biol. Biochem.* **2014**, *70*, 113–122. [\[CrossRef\]](#)
44. Yang, X.T.; Ning, G.H.; Dong, H.Y.; Li, Y. Soil microbial characters under different vegetation communities in Taihang Mountain area. *Chin. J. Appl. Ecol.* **2006**, *17*, 1761–1764.
45. Niu, X.Y.; Liu, Z.Q.; Zhao, J.J.; Wang, Y.Q.; Chen, Y.Q.; Du, H.; Zhang, C.F. Impact of forest succession on soil microbial diversity after fire in Greater Khingan Mountains. *Microbiology* **2017**, *44*, 1825–1833. [\[CrossRef\]](#)
46. Carnovale, D.; Bissett, A.; Thrall, P.H.; Baker, G. Plant genus (*Acacia* and *Eucalyptus*) alters soil microbial community structure and relative abundance within revegetated shelterbelts. *Appl. Soil Ecol.* **2019**, *133*, 1–11. [\[CrossRef\]](#)
47. Li, P.; Shi, R.J.; Zhao, F.; Yu, J.H.; Cui, X.Y.; Hu, J.G.; Zhang, Y. Soil bacterial community structure and predicted functions in the larch forest during succession at the Greater Khingan Mountains of Northeast China. *Chin. J. Appl. Ecol.* **2019**, *30*, 95–107. [\[CrossRef\]](#)
48. Preem, J.K.; Truu, J.; Truu, M.; Mander, U.; Oopkaup, K.; Lohmus, K.; Helmisaari, H.S.; Uri, V.; Zobel, M. Bacterial community structure and its relationship to soil physico-chemical characteristics in alder stands with different management histories. *Ecol. Eng.* **2012**, *49*, 10–17. [\[CrossRef\]](#)
49. Lauber, C.L.; Strickland, M.S.; Bradford, M.A.; Fierer, N. The influence of soil properties on the structure of bacterial and fungal communities across land-use types. *Soil Biol. Biochem.* **2008**, *40*, 2407–2415. [\[CrossRef\]](#)
50. Zhao, B.X.; Pan, F.R.; Han, X.R. Bacterial community development based on Illumina amplicon sequencing of 16S rDNA in the cherry rhizosphere. *Chin. J. Soil Sci.* **2018**, *49*, 596–601. [\[CrossRef\]](#)
51. Yang, L.B.; Sui, X.; Cui, F.X.; Zhu, D.G.; Song, H.L.; Ni, H.W. Soil bacterial diversity between different forest wet successional stages in Tangwanghe National Park. *Res. Environ. Sci.* **2019**, *32*, 458–464. [\[CrossRef\]](#)
52. Kang, H.Z.; Gao, H.H.; Yu, W.J.; Yi, Y.; Wang, Y.; Ning, M.L. Changes in soil microbial community structure and function after afforestation depend on species and age: Case study in a subtropical alluvial island. *Sci. Total Environ.* **2018**, *625*, 1423–1432. [\[CrossRef\]](#) [\[PubMed\]](#)
53. Kim, S.; Zang, H.D.; Mortimer, P.; Shi, L.L.; Li, Y.J.; Xu, J.C.; Ostermann, A. Tree species and recovery time drives soil restoration after mining: A chronosequence study. *Land Degrad. Dev.* **2018**, *29*, 1738–1747. [\[CrossRef\]](#)
54. Lauber, C.L.; Hamady, M.; Knight, R.; Fierer, N. Pyrosequencing-based assessment of soil pH as a predictor of soil bacterial community structure at the continental scale. *Appl. Environ. Microbiol.* **2009**, *75*, 5111–5120. [\[CrossRef\]](#) [\[PubMed\]](#)
55. Navarrete, A.A.; Kuramae, E.E.; de Hollander, M.; Pijl, A.S.; van Veen, J.A.; Tsai, S.M. Acidobacterial community responses to agricultural management of soybean in Amazon forest soils. *FEMS Microbiol. Ecol.* **2013**, *83*, 607–621. [\[CrossRef\]](#) [\[PubMed\]](#)
56. DeBruyn, J.M.; Nixon, L.T.; Fawaz, M.N.; Johnson, A.M.; Radosevich, M. Global Biogeography and Quantitative Seasonal Dynamics of Gemmatimonadetes in Soil. *Appl. Environ. Microb.* **2011**, *77*, 6295–6300. [\[CrossRef\]](#) [\[PubMed\]](#)

57. Myers, J.A.; Chase, J.M.; Jiménez, I.; Jørgensen, P.M.; Araujo-Murakami, A.; Paniagua-Zambrana, N.; Seidel, R.; Cornell, H. Beta-diversity in temperate and tropical forests reflects dissimilar mechanisms of community assembly. *Ecol. Lett.* **2013**, *16*, 151–157. [[CrossRef](#)] [[PubMed](#)]
58. Ren, C.J.; Zhao, F.Z.; Kang, D.; Yang, G.H.; Han, X.H.; Tong, X.G.; Feng, Y.Z.; Ren, G.X. Linkages of C:N:P stoichiometry and bacterial community in soil following afforestation of former farmland. *Forest Ecol. Manag.* **2016**, *376*, 59–66. [[CrossRef](#)]
59. Gunina, A.; Smith, A.R.; Godbold, D.L.; Jones, D.L.; Kuzyakov, Y. Response of soil microbial community to afforestation with pure and mixed species. *Plant Soil* **2017**, *412*, 357–368. [[CrossRef](#)]
60. Bardgett, R.; Wardle, D.A. Aboveground-belowground linkages: Biotic interactions, ecosystem processes, and global change. *Eos Trans. Am. Geophys. Union* **2011**, *92*, 222. [[CrossRef](#)]
61. Kaiser, K.; Wemheuer, B.; Korolkow, V.; Wemheuer, F.; Nacke, H.; Schoning, I.; Schrumpf, M.; Daniel, R. Driving forces of soil bacterial community structure, diversity, and function in temperate grasslands and forests. *Sci. Rep. UK* **2016**, *6*, 33696. [[CrossRef](#)] [[PubMed](#)]
62. Bezemer, T.M.; Fountain, M.T.; Barea, J.M.; Christensen, S.; Dekker, S.C.; Duyts, H.; van Hal, R.; Harvey, J.A.; Hedlund, K.; Maraun, M. Divergent composition but similar function of soil food webs of individual plants: Plant species and community effects. *Ecology* **2010**, *91*, 3027–3036. [[CrossRef](#)]
63. Li, S.J.; Zhu, T.H.; Liu, Z.X. Effects of two models of forest rehabilitation on dominant groups of soil microbes. *Bull. Soil Water Conserv.* **2014**, *34*, 186–191. [[CrossRef](#)]
64. Palomo, A.; Pedersen, A.G.; Fowler, S.J.; Dechesne, A.; Sicheritz-Pontén, T.; Smets, B.F. Comparative genomics sheds light on niche differentiation and the evolutionary history of comammox *Nitrospira*. *ISME J.* **2017**, *12*, 1779–1793. [[CrossRef](#)]
65. Ushiki, N.; Jinno, M.; Fujitani, H.; Suenaga, T.; Terada, A.; Tsuneda, S. Nitrite oxidation kinetics of two *Nitrospira* strains: The quest for competition and ecological niche differentiation. *J. Biosci. Bioeng.* **2017**, *123*, 581–589. [[CrossRef](#)] [[PubMed](#)]
66. Castaneda, L.E.; Barbosa, O. Metagenomic analysis exploring taxonomic and functional diversity of soil microbial communities in Chilean vineyards and surrounding native forests. *PeerJ* **2017**, *5*, e3098. [[CrossRef](#)]
67. Finlay, B.J.; Clarke, K.J. Ubiquitous dispersal of microbial species. *Nature* **1999**, *400*, 828. [[CrossRef](#)]
68. Xu, F.; Cao, F.Q.; Kong, Q.; Zhou, L.L.; Yuan, Q.; Zhu, Y.J.; Wang, Q.; Du, Y.D.; Wang, Z.D. Electricity production and evolution of microbial community in the constructed wetland-microbial fuel cell. *Chem. Eng. J.* **2018**, *339*, 479–486. [[CrossRef](#)]
69. Gelaw, A.M.; Singh, B.R.; Lal, R. Soil organic carbon and total nitrogen stocks under different land uses in a semi-arid watershed in Tigray, Northern Ethiopia. *Agric. Ecosyst. Environ.* **2014**, *188*, 256–263. [[CrossRef](#)]
70. Yan, X.Y.; Cai, Z.C.; Wang, S.W.; Smith, P. Direct measurement of soil organic carbon content change in the croplands of China. *Glob. Chang. Biol.* **2011**, *17*, 1487–1496. [[CrossRef](#)]
71. Cao, X.B.; Lin, D.; Cai, L.; Jiang, Y.M.; Zhu, D. Effects of different vegetation communities on soil carbon fraction, RubisCO activity and cbbl genes in Nanjishan wetland of Poyang Lake. *Acta Pedol. Sin.* **2017**, *54*, 1269–1279. [[CrossRef](#)]
72. Claus, H. Laccases: Structure, reactions, distribution. *Micron* **2004**, *35*, 93–96. [[CrossRef](#)] [[PubMed](#)]
73. Ebersberger, D.; Niklaus, P.A.; Kandeler, E. Long term CO₂ enrichment stimulates N-mineralisation and enzyme activities in calcareous grassland. *Soil Biol. Biochem.* **2003**, *35*, 965–972. [[CrossRef](#)]
74. Liang, B.C.; Wang, X.L.; Ma, B.L. Maize root-induced change in soil organic carbon pools. *Soil Sci. Soc. Am. J.* **2002**, *66*, 845–847. [[CrossRef](#)]
75. Lu, J.L.; Shen, G.; Wang, Q.; Ren, M.L.; Pei, Z.X.; Wei, C.H.; Wang, W.J. Effect of urban tree species on soil physicochemical properties in Harbi, Northeastern China, and afforestation implications. *Bull. Bot. Res.* **2016**, *36*, 549–555. [[CrossRef](#)]
76. Wang, W.B.; Wang, Y.P.; Wang, H.T.; Ma, X.S.; Yi, W.H. Effects of different continuous cropping and rotation of poplar plantation on soil nitrogen bacteria community and nitrogen metabolism. *Sci. Silvae Sin.* **2016**, *52*, 45–54. [[CrossRef](#)]
77. Yoon, S.; Cruz-Garcia, C.; Sanford, R.; Ritalahti, K.M.; Löffler, F.E. Denitrification versus respiratory ammonification: Environmental controls of two competing dissimilatory NO₃[−]/NO₂[−] reduction pathways in *Shewanella loihica* strain PV-4. *ISME J.* **2015**, *9*, 1093–1104. [[CrossRef](#)]

78. Bent, E.; Nemeth, D.; Wagner-Riddle, C.; Dunfield, K. Residue management leading to higher field-scale N_2O flux is associated with different soil bacterial nitrifier and denitrifier gene community structures. *Appl. Soil Ecol.* **2016**, *108*, 288–299. [[CrossRef](#)]
79. Kyaing, S.M.; Gu, L.H.; Cheng, H.M. The role of nitrate reductase and nitrite reductase in plant. *Curr. Biotechnol.* **2011**, *1*, 159–164. [[CrossRef](#)]
80. Li, X.B.; Xia, L.L.; Yan, X.Y. Application of membrane inlet mass spectrometry to directly quantify denitrification in flooded rice paddy soil. *Biol. Fertil. Soils* **2014**, *50*, 891–900. [[CrossRef](#)]
81. Ma, X.S.; Wang, W.B.; Wang, Y.P.; Wang, H.T.; Yi, W.H. Characteristics of phosphate-solubilizing microbial community in the soil of poplar plantations under successive-planting and rotation. *Chin. J. Appl. Ecol.* **2016**, *27*, 1877–1885. [[CrossRef](#)]
82. Schachtman, D.P.; Reid, R.J.; Ayling, S.M. Phosphorus uptake by plants: From soil to cell. *Plant Physiol.* **1998**, *116*, 447–453. [[CrossRef](#)] [[PubMed](#)]
83. Krey, T.; Vassilev, N.; Baum, C.; Eichler-Löbermann, B. Effects of long-term phosphorus application and plant-growth promoting rhizobacteria on maize phosphorus nutrition under field conditions. *Eur. J. Soil Biol.* **2013**, *55*, 124–130. [[CrossRef](#)]
84. Tang, W.P.; Li, J.Y.; Qi, L.H.; Hu, X.Y.; Cui, H.X. Effects of poplar successive plantation on soil chemical characteristics in Jiangnan Plain. *J. Cent. South Univ. For. Technol.* **2009**, *29*, 72–76.
85. Wu, Y.; Wang, W.J.; Wang, Q.; Zhong, Z.L.; Pei, Z.X.; Wang, H.M.; Yao, Y.L. Impact of poplar shelterbelt plantations on surface soil properties in northeastern China. *Can. J. Forest Res.* **2018**, *48*, 559–567. [[CrossRef](#)]
86. Chang, L.F. *Isolation, Purification and Properties of APS Reductase and Sulfate Reductase from Sulfate-Reducing Bacterium*; Inner Mongolia Normal University: Huhehaote, China, 2008.
87. Bick, J.A.; Dennis, J.J.; Zylstra, G.J.; Nowack, J.; Leustek, T. Identification of a new class of 5'-adenylylsulfate (APS) reductases from sulfate-assimilating bacteria. *J. Bacteriol.* **2000**, *182*, 135–142. [[CrossRef](#)]
88. Biderre Petit, C.; Boucher, D.; Kuever, J.; Alberic, P.; Jézéquel, D.; Chebance, B.; Borrel, G.; Fonty, G.; Peyret, P. Identification of sulfur-cycle prokaryotes in a low-sulfate lake (Lake Pavin) using *aprA* and 16S rRNA gene markers. *Microb. Ecol.* **2011**, *61*, 313–327. [[CrossRef](#)]
89. Nair, A.; Ngouajio, M. Soil microbial biomass, functional microbial diversity, and nematode community structure as affected by cover crops and compost in an organic vegetable production system. *Appl. Soil Ecol.* **2012**, *58*, 45–55. [[CrossRef](#)]
90. Kubartova, A.; Moukoudi, J.; Beguiristain, T.; Ranger, J.; Berthelin, J. Microbial diversity during cellulose decomposition in different forest stands: I. Microbial communities and environmental conditions. *Microb. Ecol.* **2007**, *54*, 393–405. [[CrossRef](#)]
91. Bergkemper, F.; Welzl, G.; Lang, F.; Krüger, J.; Schloter, M.; Schulz, S. The importance of C, N and P as driver for bacterial community structure in German beech dominated forest soils. *J. Plant Nutr. Soil. Sci.* **2016**, *179*, 472–480. [[CrossRef](#)]

